TRX-1 Regulates SKN-1 Nuclear Localization Cell Non-autonomously in *Caenorhabditis elegans*

Katie C. McCallum,*,† Bin Liu,‡,§ Juan Carlos Fierro-González, Peter Swoboda,** Swathi Arur,†,‡,§ Antonio Miranda-Vizuete,††,1,2 and Danielle A. Garsin*,†,1,2**

*Department of Microbiology and Molecular Genetics, The University of Texas Health Science Center, Houston, Texas 77030, †The University of Texas Graduate School of Biomedical Sciences, Houston, Texas 77030, ‡Department of Genetics and §Center for Genetics and Genomics, Department of Genetics, The University of Texas MD Anderson Cancer Center, Houston, Texas 77030, **Department of Biosciences and Nutrition at Novum, Karolinska Institute, S-141 83 Huddinge, Sweden, and ††Instituto de Biomedicina de Sevilla, Hospital Universitario Virgen del Rocío/Consejo Superior de Investigaciones Cientfícas/Universidad de Sevilla, E-41013 Sevilla, Spain

ORCID ID: 0000-0002-6856-5396 (A.M.-V.)

ABSTRACT The *Caenorhabditis elegans* oxidative stress response transcription factor, SKN-1, is essential for the maintenance of redox homeostasis and is a functional ortholog of the Nrf family of transcription factors. The numerous levels of regulation that govern these transcription factors underscore their importance. Here, we add a thioredoxin, encoded by *trx-1*, to the expansive list of SKN-1 regulators. We report that loss of *trx-1* promotes nuclear localization of intestinal SKN-1 in a redox-independent, cell non-autonomous fashion from the ASJ neurons. Furthermore, this regulation is not general to the thioredoxin family, as two other *C. elegans* thioredoxins, TRX-2 and TRX-3, do not play a role in this process. Moreover, TRX-1-dependent regulation requires signaling from the p38 MAPK-signaling pathway. However, while TRX-1 regulates SKN-1 nuclear localization, classical SKN-1 transcriptional activity associated with stress response remains largely unaffected. Interestingly, RNA-Seq analysis revealed that loss of *trx-1* elicits a general, organism-wide down-regulation of several classes of genes; those encoding for collagens and lipid transport being most prevalent. Together, these results uncover a novel role for a thioredoxin in regulating intestinal SKN-1 nuclear localization in a cell non-autonomous manner, thereby contributing to the understanding of the processes involved in maintaining redox homeostasis throughout an organism.

KEYWORDS *Caenorhabditis elegans*; oxidative stress response; thioredoxin; ASJ neurons; cell non-autonomous signaling

THE ability of an organism to maintain redox homeostasis is critical for its survival. At the cellular level, exposure to oxidative insult can irreversibly damage DNA, proteins, and lipids, all of which can lead to cell apoptosis or necrosis (Ray *et al.* 2012; Thanan *et al.* 2014). At the organismal level, unresolved oxidative stress is considered a hallmark of numerous life-threatening diseases, including Alzheimer's, Parkinson's disease, atherosclerosis, and several forms of cancer (Hybertson *et al.* 2011; Thanan *et al.* 2014). To counteract oxidative insults, organisms have evolved specific pathways capable of sensing and responding to both endogenous and exogenous oxidative stress, termed "the oxidative stress response" (Lushchak 2011). This response is coordinated by oxidative stress response transcription factors, which activate the expression of detoxification and repair enzymes (McCord and Fridovich 1969; Anderson 1998; Lushchak 2011). In mammals, the major oxidative stress transcription factor is the nuclear factor erythroid 2-related factor, Nrf2, one of three Nrf paralogs (Hybertson *et al.* 2011). To ensure efficient surveillance of redox homeostasis, several mechanisms regulate Nrf2, including those that regulate its subcellular localization and protein turnover (Marinho *et al.* 2014).

The nematode *Caenorhabditis elegans* utilizes a functional ortholog of mammalian Nrf proteins, SKN-1, to coordinate its oxidative stress response (Walker *et al.* 2000; An and Blackwell 2003). More recently, a role for SKN-1 has been

doi: 10.1534/genetics.115.185272
Manuscript received November 24, 2015; accepted for publication February 22, 2016; published Early Online February 24, 2016.
Supplemental material is available online at www.genetics.org/lookup/suppl/doi:10.1534/genetics.115.185272/-/DC1.
[1]These authors contributed equally to this work.
[2]Corresponding authors: University of Texas Health Science Center, Department of Microbiology and Molecular Genetics, P.O. Box 20708, 6431 Fannin St./MSB 1.168 Houston, TX 77030. E-mail: danielle.a.garsin@uth.tmc.edu; Instituto de Biomedicina de Sevilla–IBiS, Laboratorio 118, Campus del Hospital Universitario Virgen del Rocío, Avda. Manuel Siurot s/n, 41013 Sevilla, Spain. E-mail: amiranda-ibis@us.es

found in the regulation of the unfolded protein response and the maintenance of lipid homeostasis (Glover-Cutter *et al.* 2013; Lynn *et al.* 2015; Steinbaugh *et al.* 2015). Similar to Nrf2, SKN-1 regulation is also well studied, and overlapping mechanisms of regulation exist between mammals and worms. In general, both Nrf2 and SKN-1 seem to be regulated at the level of nuclear accumulation. Specifically, both mammals and worms employ cysteine-rich adaptor proteins, Keap1 and WDR-23, respectively, to facilitate the degradation of these transcription factors by the proteasome, thereby preventing their nuclear accumulation (Choe *et al.* 2009; Leung *et al.* 2014; Marinho *et al.* 2014). Furthermore, both mammalian and worm glycogen synthase kinase 3 phosphorylate Nrf2 and SKN-1, respectively, in a manner that impacts the subcellular localization of these transcription factors (An *et al.* 2005; Salazar *et al.* 2006). In *C. elegans*, additional mechanisms of SKN-1 regulation were elucidated. SKN-1 isoform C is antagonized by insulin/IGF-1-like signaling and is positively regulated by the p38 MAPK pathway via phosphorylation of Serines 74 and 340 (Inoue *et al.* 2005; Tullet *et al.* 2008). Exposure to oxidative stressors, such as sodium arsenite, impact these positive and negative regulators governing intestinal SKN-1, resulting in increased nuclear localization and transcriptional activation, thereby maintaining redox homeostasis (Inoue *et al.* 2005). However, while many factors and mechanisms of regulating SKN-1 are known, how these signaling pathways initially sense oxidative imbalance remains unclear.

Thioredoxins are small proteins that, due to their inherent amino acid chemistry, are redox reactive (Arner and Holmgren 2000; Powis and Montfort 2001; Buchanan *et al.* 2012). While thioredoxins can act as antioxidants via their ability to reduce oxidized proteins, they play a prominent role in the regulation of signaling pathways in several organisms (Fujino *et al.* 2006; Yoshioka *et al.* 2006). In mammals, thioredoxin 1, TRX1, serves as an allosteric inhibitor of apoptosis signal-regulating kinase 1, ASK1, by preventing dimerization at the N terminus of this MAPKKK, thereby inhibiting activation of p38 MAPK pathway signaling. Upon oxidation of TRX1 by reactive oxygen species (ROS), repression of ASK1 is relieved and ASK1 is able to homodimerize, activating its kinase activity and ultimately triggering the apoptotic response (Fujino *et al.* 2007). While the redox activity of thioredoxin is important for a majority of its cellular functions, thioredoxins have important, redox-independent cellular roles. For example, TRX1 promotes ASK1 ubiquitination and degradation irrespective of its redox activity (Liu and Min 2002). Moreover, a *C. elegans* thioredoxin, TRX-1, modulates DAF-28 signaling during dauer formation in a redox-independent fashion (Fierro-Gonzalez *et al.* 2011a).

In *C. elegans*, TRX-1 plays a role in life span, dauer formation, dietary restriction, and the oxidative stress response (Jee *et al.* 2005; Miranda-Vizuete *et al.* 2006; Fierro-Gonzalez *et al.* 2011a,b). However, no specific role for thioredoxins in signaling has been characterized in the worm. Given the general ability of thioredoxins to act as both redox-dependent and redox-independent regulators and for mammalian TRX1 to regulate the p38 MAPK pathway, we reasoned that a thioredoxin may regulate SKN-1 and/or the *C. elegans* oxidative stress response.

In this work, we explore whether thioredoxins are regulators of SKN-1 or one of the previously characterized SKN-1 regulatory components. Interestingly, we demonstrate that TRX-1, but not TRX-2 or TRX-3 (Cacho-Valadez *et al.* 2012; Jimenez-Hidalgo *et al.* 2014), affects the nuclear localization of intestinal SKN-1. Specifically, we observed that the nuclear localization of intestinal SKN-1 is increased in a *trx-1(ok1449)* null mutant and that this *trx-1*-dependent localization does not require redox activity but does require the p38 MAPK pathway. TRX-1 expression is restricted to the ASJ neurons (Jee *et al.* 2005; Miranda-Vizuete *et al.* 2006), indicating cell non-autonomous regulation and arguing against a direct interaction of TRX-1 with SKN-1 or its regulatory components. Nuclear localization of intestinal SKN-1 usually parallels activation of SKN-1-regulated genes, but we found by quantitative real time PCR (qRT-PCR) and RNA-Seq that loss of *trx-1* did not increase the typical transcriptional activity of SKN-1 (An *et al.* 2005; Inoue *et al.* 2005; Tullet *et al.* 2008; Choe *et al.* 2009; Leung *et al.* 2014). Rather than an upregulation of the oxidative stress response transcriptional program, a downregulation of many genes was observed, particularly those encoding collagen and lipid transport and localization proteins. Interestingly, only three genes (*lips-6*, *lips-11*, and *lbp-8*), encoding two lipase-related proteins and a lipid chaperone, respectively, are up-regulated upon loss of *trx-1*. In summary, the data presented support a model in which nuclear localization, but not activation, of intestinal SKN-1 is regulated cell non-autonomously by TRX-1 in a redox-independent fashion.

Materials and Methods

Strains

C. elegans strains were grown and maintained as previously described (Hope 1999). *C. elegans* strains used in this study are listed in Supplemental Material, Table S4. The following bacterial strains were used in this study: *Escherichia coli* OP50, Enterococcus *faecalis* OG1RF, Pseudomonas *aeruginosa* PA14, and *E. coli* HT115.

Strain construction

In general, all mutant strains were backcrossed to wild-type N2 6x. To generate the VZ27, VZ26, and VZ157 strains, *Is007 [skn-1b/c::gfp; rol-6(su1006)]* worms were crossed with *trx-1(ok1449)*, *trx-2(tm2720)*, and *trx-3(tm2820)* mutants, respectively. To visualize TRX-1 localization, the OE3381 strain was generated by injecting the pPD95.77 plasmid containing *trx-1* (1-kb promoter + gene) fused to *gfp* with the *trx-1* 3′ UTR (rather than the *unc-54* 3′ UTR native to this vector). To generate the VZ472, VZ458, and VZ461 strains, the *trx-1* promoter was replaced with tissue-specific promoters (*ssu-1*; ASJ, *ges-1*; intestinal, *daf-7*; ASI) in the above-mentioned plasmid. These constructs were then injected into wild-type N2 worms along with the *Punc-122*::*DsRed* coinjection marker that causes red fluorescence in the coelomocytes. Finally, the arrays were transferred into the *trx-1(ok1449)*; *Is007* background to generate GF92, GF93, and GF94 strains, respectively. To determine p38 MAPK-signaling dependence, *nsy-1(ok593)*, *sek-1(km4)*, and *pmk-1(km25)* mutants were crossed into the *trx-1(ok1449)*; *Is007* background to generate the GF96, GF97, and GF98 strains, respectively. *Ex060[skn-1(S74,340A)b/c*::*gfp; rol-6(su1006)]* was also crossed into the *trx-1(ok1449)*; *Is007* background to further verify p38 MAPK-signaling dependence (GF95). To visualize *gst-4* expression in the *trx-1* background, the VZ433 strain was made by crossing *trx-1(ok1449)* mutants with *dvIs19 [Pgst-4*::*gfp*::*NLS*; *rol-6(su1006)]* worms. To generate GF99 and GF100, OE4064 and OE4067 were crossed into the *trx-1(ok1449)*; *Is007* background and maintained at 25° for four generations to remove the *daf-28(sa191)* mutation.

RNA interference

To knock down *skn-1* expression, RNA interference (RNAi) was induced by feeding L1- to L4-stage worms with bacteria producing *skn-1* double-stranded RNA. The *skn-1* RNAi bacterial strain was made previously, as described (Hoeven *et al.* 2011).

Fluorescence microscopy

To visualize SKN-1B/C::GFP and TRX-1::GFP localization and *gst-4::gfp* expression, young adults were washed from plates and anesthetized with 1 mM levamisole. Anesthetized worms were mounted on 2% agarose pads and visualized and imaged using Olympus IX81 automated inverted microscope and Slidebook (version 5.0) software. For SKN-1B/C::GFP localization quantification, the percentage of intestinal SKN-1B/C::GFP nuclear localization was categorically scored as follows: none: no localization; low: posterior or anterior intestinal localization; medium: posterior and anterior intestinal localization; high: localization throughout the entire intestine (Inoue *et al.* 2005). For GF99 and GF100, percentage of intestinal SKN-1B/C::GFP nuclear localization was categorically scored in an area limited to the anterior intestine of animals as follows: none: no localization; low: weak fluorescence; medium: moderate fluorescence; or high: bright fluorescence. Chi square and Fisher's exact tests (GraphPad Prism version 5.0) were used to calculate significance of SKN-1B/C::GFP nuclear localization averaged between three biological replicates of $n \geq 50$ worms.

Western blotting

About 1000 worms were washed from NGM plates and collected in a 100-μl pellet using protein extraction buffer [50 mM Tris, pH 7.5, 50 mM NaCl, protease inhibitor cocktail (Roche, 11873580001), PhosStop (Roche, 04906845001)]. The pellet was sonicated (on ice) for 10 sec at level 5 and 50% duty. Suspensions were incubated in 1% SDS on ice for 5 min and then centrifuged in the cold at 14,000 × *g* for 10 min. Supernatants were transferred to a fresh Eppendorf tube, and total protein concentration was measured via BCA assay (Pierce, 23227). Sample buffer was added and protein lysates were boiled for 5 min. For SKN-1C detection, total protein was separated using a 10% SDS-PAGE gel with 15 μg of total protein per well. The gel was transferred to a nitrocellulose membrane for 60 min at 4°. The membrane was blocked in 5% milk + TBST for 1 hr at room temperature. The membrane was then incubated with 1:200 monoclonal SKN-1 antibody (FC4) overnight at 4° (Bowerman *et al.* 1993). The blot was washed eight times for 5-min intervals with TBST. The blot was then incubated with 1:1000 secondary HRP-conjugated anti-mouse antibody for 30 min and subsequently washed eight times for 5-min intervals. Blots were developed using SuperSignal West Dura Extended Duration Substrate (Pierce, 37071) and visualized using an ImageQuant LAS 4000 imager (GE Healthcare Life Sciences). Note that we were unable to detect SKN-1C::GFP and that there are presently no examples in the literature of successful detection of the fusion protein with this antibody. For phospho-NSY-1 detection, total protein was separated using an 8% SDS-PAGE gel with at least 70 μg of total protein per well. The gel was transferred to a nitrocellulose membrane for 75 min at 4°. The membrane was blocked in 5% BSA + TBST overnight at 4°. The membrane was then incubated with 1:1000 Phospho-ASK1 (Thr845) Antibody (Cell Signaling, #3765) or Phospho-p38 MAPK (Thr180/Tyr182) Antibody (Cell Signaling, #9211) for 5.5 hr at 4°. The blot was washed four times for 5-min intervals with TBST. The blot was then incubated with 1:3000 secondary HRP-conjugated anti-mouse antibody (for anti-ASK1 blot) or 1:5000 secondary HRP-conjugated anti-rabbit antibody (for anti-p38 blot) for 30 min and subsequently washed four times for 5-min intervals. Blots were developed as above. Both blots were repeated at least three times, obtaining similar results. Anti-α-tubulin was used as a loading control with a 1-hr incubation in 1:1000 primary antibody (Sigma, T9026) concentration and a 30-min incubation in 1:3000 goat anti-rabbit HRP-conjugated secondary antibody with similar washing procedures as described above.

Oxidative stress and killing assays

To assess sensitivity to oxidative stress, sodium arsenite ($NaAsO_2$) was added to NGM plates to a final concentration of 10 mM. Overnight *E. coli* OP50 culture was generously seeded and incubated for growth (at 37°) on $NaAsO_2$ plates. For microscopy, qRT-PCR, and Western blotting, ~1000 worms were incubated on $NaAsO_2$ plates for 5 hr at 20°. For survival assays, 90 worms were added to three replicate plates and scored hourly for survival. To assess sensitivity to pathogen stress, killing assays were performed as previously described, with slight modification (Mahajan-Miklos *et al.*

1999; Garsin *et al.* 2001). *E. faecalis* OG1RF grown in BHI for 5 hr was seeded onto BHI plates and grown overnight at 37°. *P. aeruginosa* PA14 grown in LB for 8 hr was seeded onto SK plates and grown overnight at 37°. A total of 90 worms were added to three replicate plates of each pathogen and scored for survival at various times points over the course of the assay. Kaplan–Meier log-rank analysis was used to compare the significance of the survival curves using median survival.

qRT-PCR analysis

Using TRIzol (Invitrogen), RNA was extracted (as directed by the manufacturer) from young adult worms exposed or left unexposed to sodium arsenite and analyzed via qRT-PCR, as previously described (Hoeven *et al.* 2011). The average gene expression of biological triplicates was graphed, and error bars represent the standard error of the mean (SEM). A paired Student's *t*-test was used to determine significance where indicated. Primers used in this approach are listed in Table S5.

RNA sequencing

Young adult animals were incubated on NGM plates with and without 10 mM sodium arsenite for 5 hr, at which point total RNA was extracted (as described above) and sent for RNA sequencing (RNA-Seq). There were an average 101,140,446 reads/sample generated from the RNA-Seq. The average percentage of the bases with ≥Q30 reads was 90.1%. We used the *C.elegans* genome (version ce10) as the reference that can be downloaded from the iGenome databases (ftp://igenome:G3nom3s4u@ussd-ftp.illumina.com/Caenorhabditis_elegans/UCSC/ce10/Caenorhabditis_elegans_UCSC_ce10.tar.gz). The sequencing reads were mapped to the genome with the application TopHat (Trapnell *et al.* 2012; Trapnell *et al.* 2013), which utilizes the high-throughput sequence aligner bowtie (Langmead *et al.* 2009). The application Cufflinks further processed the transcripts assembly and the abundance estimation. The FPKMs (Fragments Per Kilobase of transcript per Million mapped reads) were calculated for the gene differential expression analysis. To visualize the results generated from Cufflinks, we used an R/Bioconductor package CummeRbund (http://bioconductor.org). Venn diagrams generated by R programming enabled the affected gene comparison between samples. To explore the functional groups for the differentially expressed genes, we further carried out the Gene Ontology (GO) analysis with the application Database for Annotation, Visualization and Integrated Discovery (Huang da *et al.* 2009a,b). The three subontologies (MF: molecular function; BP: biological process; and CC: cellular component) were assessed.

Data availability

All strains are available upon request. Table S4 contains genotypes for each strain used in this study. Table S5 contains nucleotide sequences for each primer used in qRT analysis. RNA-Seq gene expression data are available in Table S6 or at *Gene Expression Omnibus* under accession no. GSE77976.

Results

TRX-1 negatively regulates SKN-1 nuclear localization

Previously, we identified a role for SKN-1 in the *C. elegans* immune response. We found that the *C. elegans* dual oxidase, Ce-Duox1/BLI-3, is responsible for the purposeful production of ROS as a means of combatting bacterial infection (Chavez *et al.* 2009). In a follow-up study, we demonstrated that the ROS produced by BLI-3 during infection activates SKN-1-dependent expression of antioxidants in a p38 MAPK pathway-dependent manner, as a means to protect the host from the inadvertent consequences of protective ROS production (Hoeven *et al.* 2011). However, the mechanism(s) by which the p38 MAPK pathway is activated to stimulate SKN-1 remained elusive.

Given the ability of thioredoxins to regulate a variety of signaling pathways, and specifically p38 MAPK pathway activation in mammals, we wanted to determine whether thioredoxins also regulate SKN-1. Using fluorescence microscopy, we examined the ability of TRX-1, TRX-2, and TRX-3, three thioredoxins encoded by the *C. elegans* genome (Miranda-Vizuete *et al.* 2006; Cacho-Valadez *et al.* 2012; Jimenez-Hidalgo *et al.* 2014), to regulate SKN-1 nuclear localization using a well-characterized strain expressing GFP-tagged SKN-1 protein (SKN-1B/C::GFP), which has been shown to rescue *skn-1*-dependent functions (An and Blackwell 2003) Under normal conditions, with the exception of the ASI neurons where SKN-1::GFP is constitutively localized to the nuclei (white asterisk, Figure 1A), no specific expression of the GFP is detected (An and Blackwell 2003). Interestingly, however, SKN-1::GFP localizes to the nuclei of intestinal cells in *trx-1* mutants, even in the absence of stress (Figure 1, A and B). This effect was specific to *trx-1* since loss of either *trx-2* or *trx-3* does not affect intestinal SKN-1::GFP nuclear localization (Figure 1, A, C, and D). Quantification of nuclear localization of SKN-1::GFP demonstrated that loss of *trx-1* results in a threefold increase in SKN-1::GFP nuclear localization (Figure 1E). The increase in nuclear localization of intestinal SKN-1::GFP is not due to a general increase in protein levels. We assayed the protein levels of intestinal SKN-1, isoform SKN-1C, via Western analysis and found that the SKN-1C levels remain unaltered in *trx-1* null mutants compared to wild type (Figure S1). Moreover, the degree to which intestinal SKN-1::GFP nuclear localization increases upon loss of *trx-1* is similar to that seen upon exposure to the oxidative stressor, sodium arsenite (Figure S2). From this, we conclude that TRX-1 suppresses the nuclear localization of intestinal SKN-1 and therefore may be a novel negative regulator of this transcription factor.

TRX-1 regulates intestinal SKN-1 nuclear localization in a redox-independent fashion

Thioredoxins utilize a highly conserved CGPC (Cys-Gly-Pro-Cys) redox active site to reduce disulfide bonds of protein

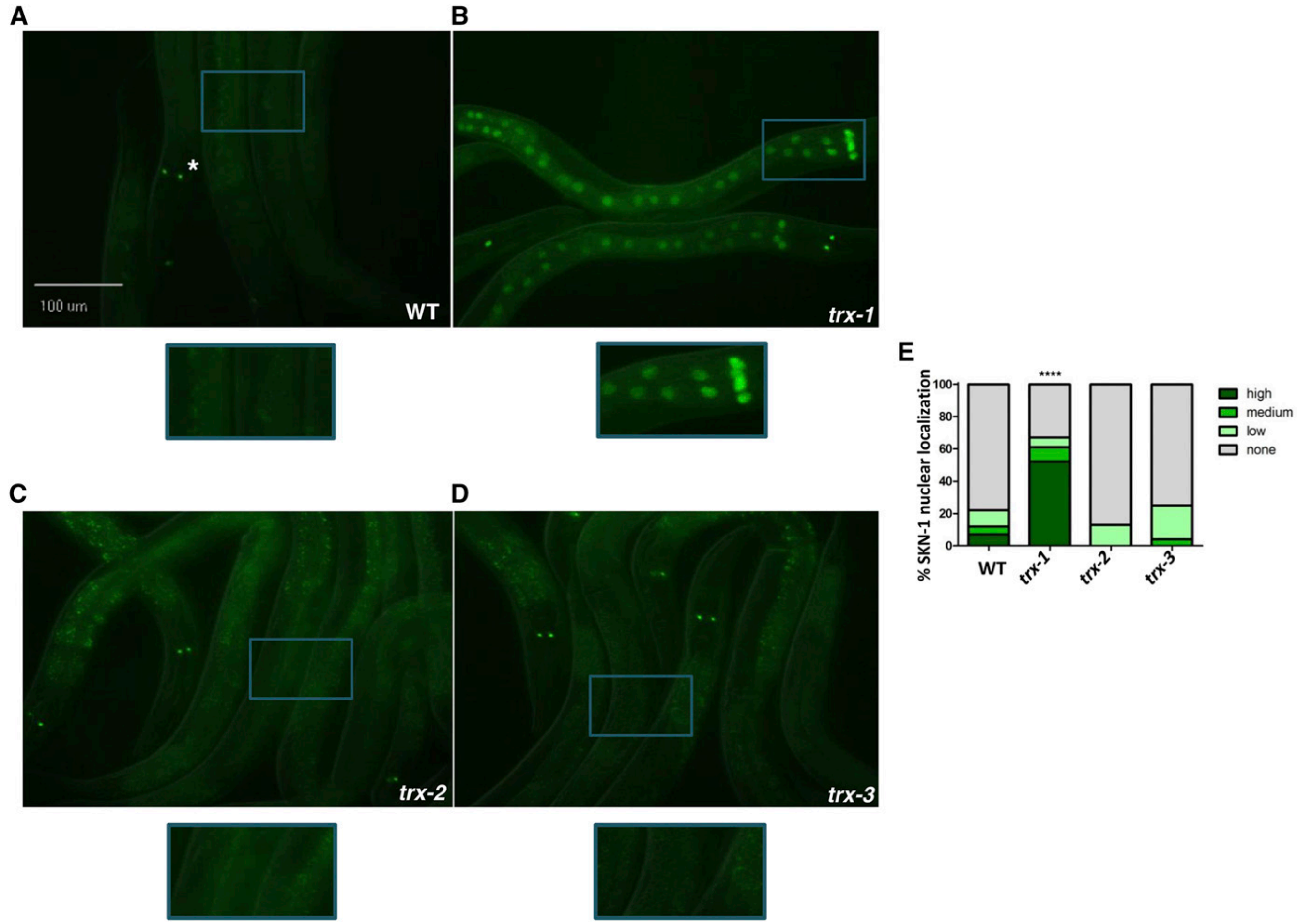

Figure 1 TRX-1 negatively regulates nuclear localization of intestinal SKN-1. (A–D) Fluorescence microscopy was used to analyze the intestinal nuclear localization of SKN-1 (SKN-1B/C::GFP) upon the loss of *trx-1*, *trx-2*, or *trx-3*. Only upon the loss of *trx-1* did SKN-1::GFP accumulate in intestinal nuclei. Asterisk in A depicts constitutive SKN-1B/C::GFP localization in the nucleus of the ASI neurons. Worms were visualized using a 20× objective. Blue boxes indicate the portion of the micrograph field that is magnified in the boxes below each micrograph. (E) Percentage of SKN-1::GFP nuclear localization was categorically scored and quantified as described in *Materials and Methods*. The percentage of SKN-1 nuclear localization increased threefold upon loss of *trx-1* (*P*-value < 0.0001 as compared to wild type). Percentages are an average of three biological replicates (n = 100 worms per replicate).

substrates (Holmgren and Lu 2010). *C. elegans* TRX-1 utilizes this redox reactive capability to reduce insulin *in vitro* (Jee *et al.* 2005; Miranda-Vizuete *et al.* 2006). However, thioredoxins also have redox-independent functions, notably in the promotion of protein folding and turnover (Berndt *et al.* 2008). Given the ability of thioredoxins to elicit both redox-dependent and redox-independent functions, we investigated whether the redox reactive residues of TRX-1 were required for its regulation of intestinal SKN-1 nuclear localization.

trx-1 mutants were complemented with either wild-type *trx-1* or "redox dead" *trx-1*, in which the redox reactive cysteines of the TRX-1 active site (CGPC) were replaced with nonreactive serine residues (SGPS) (Fierro-Gonzalez *et al.* 2011a). The transgenes were tracked using *Punc122*::*DsRed* as a co-injection marker, which labels coelomocytes with red fluorescence (Loria *et al.* 2004). Some bleed-through into the green channel resulted in the marker appearing more yellow than red in the resulting pictures (Figure 2, C and D). Under nonstressed conditions, wild-type *trx-1* restores proper SKN-1::GFP localization, similar to that seen in the *skn-1b/c*::*gfp* parent background (Figure 2, A, C, and E). Interestingly, complementation with redox dead *trx-1* restores proper SKN-1::GFP localization as well, indicating that TRX-1 regulates intestinal SKN-1::GFP nuclear localization in a redox-independent fashion (Figure 2, D and E). Upon exposure to oxidative stress, SKN-1::GFP nuclear localization was observed in both the wild-type and redox dead complements of *trx-1*, indicating that intestinal SKN-1::GFP nuclear localization is indeed inducible in these strains (Figure S3). However, the stress-induced SKN-1::GFP nuclear localization was only partially complemented, as compared to the nontransgenic backgrounds. Since complementation with transgenes often leads to overexpression, this could indicate that overproduction of TRX-1 causes it to maintain its role as a negative regulator of intestinal SKN-1::GFP nuclear localization even during stress.

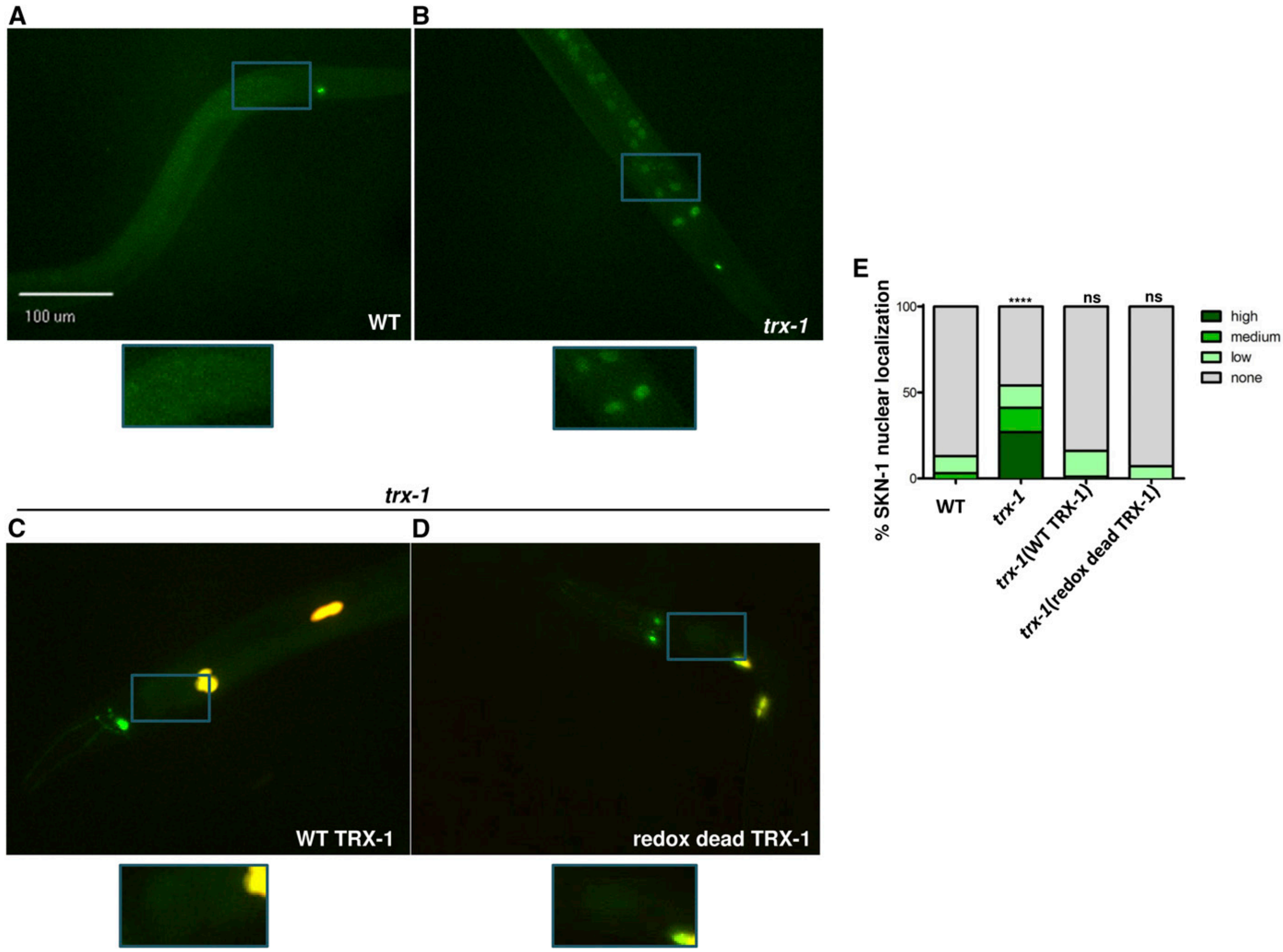

Figure 2 TRX-1 regulates intestinal SKN-1 nuclear localization in a redox-independent fashion. Fluorescence microscopy was used to analyze the intestinal nuclear localization of SKN-1::GFP in (A) wild type, (B) *trx-1* mutants, *trx-1* mutants complemented with either (C) wild-type *trx-1* or (D) redox dead *trx-1*. Worms were visualized using a 20× objective. Blue boxes indicate the portion of the micrograph field that is magnified in the boxes below each micrograph. (E) Percentage of SKN-1::GFP nuclear localization was categorically scored and quantified as described in *Materials and Methods*. While the percentage of SKN-1::GFP nuclear localization increased over twofold upon loss of *trx-1* (P-value < 0.0001), complementation with either wild-type or redox dead *trx-1* restored proper SKN-1 localization (P-value = 0.3843 and P-value = 0.1931, as compared to wild type, respectively). Percentages are an average of three biological replicates (n = 40 worms per replicate).

TRX-1 regulates SKN-1 localization cell non-autonomously from the ASJ neurons

skn-1 is constitutively expressed and localized to the nuclei of the ASI neurons and conditionally becomes localized to intestinal nuclei when worms are exposed to stress (An and Blackwell 2003). *trx-1* is expressed solely in the ASJ neurons and impacts worm longevity (Fierro-Gonzalez *et al.* 2011b; Gonzalez-Barrios *et al.* 2015). Given that the expression of *trx-1* is restricted to the ASJ neurons, but impacts intestinal SKN-1::GFP localization, we wanted to address the possibility that TRX-1 regulates intestinal SKN-1 cell non-autonomously. To assess this, we complemented the *trx-1*; *skn-1b/c*::*gfp* strain with *trx-1* expressed under the control of three separate tissue-specific promoters, *ssu-1* (ASJ neurons), *ges-1* (intestine), and *daf-7* (ASI neurons) (Edgar and McGhee 1986; Schackwitz *et al.* 1996; Carroll *et al.* 2006). To track tissue-specific rescue throughout the population, *Punc122*::*DsRed* was again used as a co-injection marker (Loria *et al.* 2004). Some bleed-through into the green channel resulted in the marker appearing more yellow than red in the resulting pictures. In Figure 3A, worms outlined in red express *trx-1* with the indicated tissue specificity, while worms outlined in white do not carry the tissue-specific rescue and display increased intestinal SKN-1 nuclear localization, thus serving as an internal control for the experiment. As evident in Figure 3A, the increased intestinal SKN-1 nuclear localization seen upon loss of *trx-1* was abolished upon specific expression of *trx-1* in the ASJ neurons, while rescue of *trx-1* expression to the intestine or ASI neurons could not restore proper intestinal SKN-1 nuclear localization.

To more quantitatively assess these observations, the percentage of SKN-1 nuclear localization was categorically scored and analyzed (Figure 3B). Loss of *trx-1* significantly

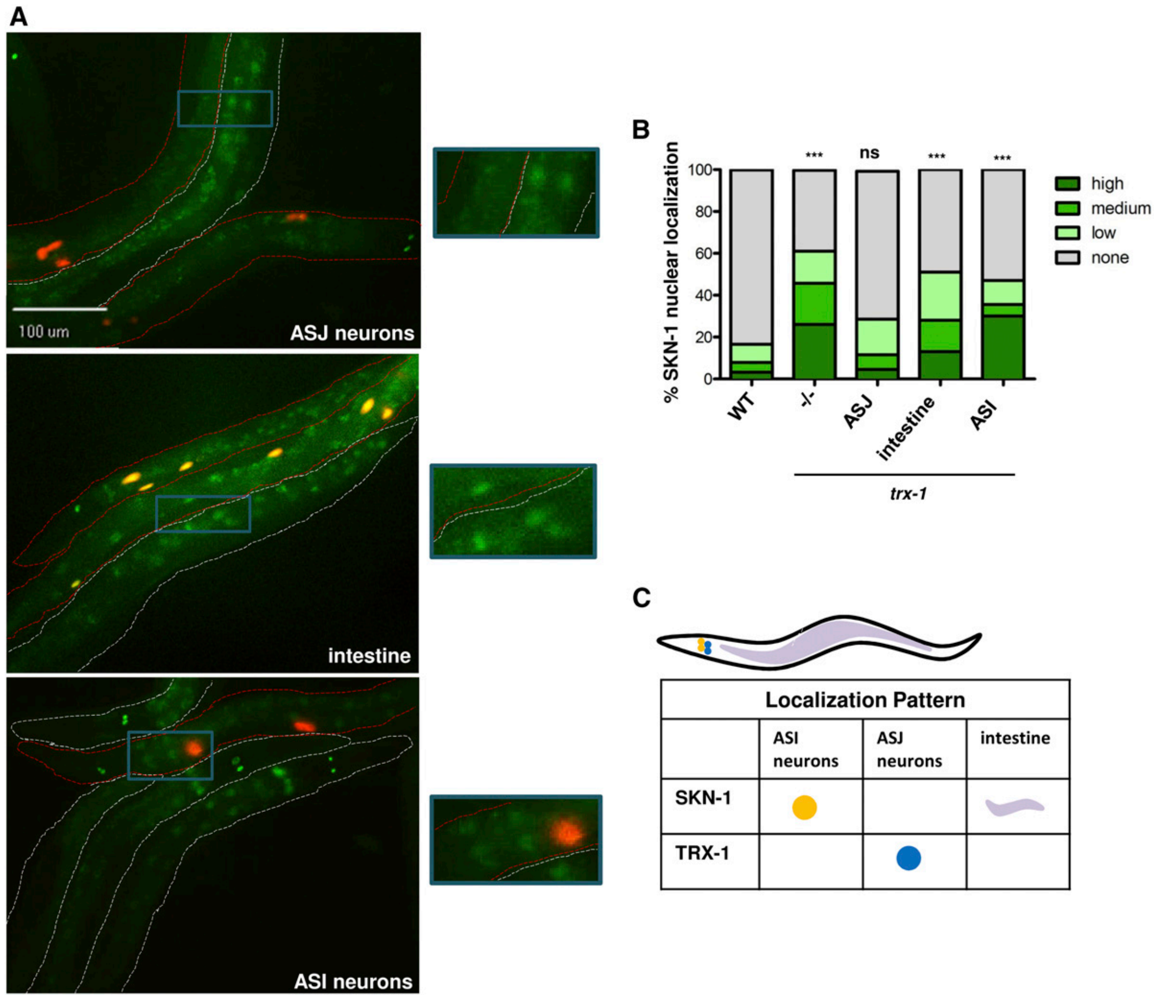

Figure 3 TRX-1 regulates SKN-1 nuclear localization cell non-autonomously. (A) Fluorescence microscopy was used to analyze intestinal SKN-1 nuclear localization upon rescue of *trx-1* expression in specific tissues in *trx-1*; *skn-1b/c*::*gfp* animals. Worms outlined in red expressed wild-type *trx-1* under the regulation of a promoter specific for the designated tissue. Nontransgenic worms (outlined in white) had a *trx-1*; *skn-1b/c*::*gfp* genotype and served as internal controls. Only expression of *trx-1* in the ASJ neurons rescued proper intestinal SKN-1::GFP nuclear localization. Worms were visualized using a 20× objective. Blue boxes indicate the portion of the micrograph field that is magnified in the boxes to the right of each micrograph. (B) Percentage of SKN-1::GFP nuclear localization was categorically scored and quantified as described in *Materials and Methods*. Percentages are an average of three biological replicates ($n \geq 35$ worms per replicate). The *trx-1* mutant exhibited a threefold increase in the percentage of intestinal SKN-1::GFP nuclear localization (*P*-value < 0.0001 as compared to wild type). The increased SKN-1::GFP nuclear localization seen upon loss of *trx-1* could be fully rescued with specific expression of *trx-1* in the ASJ neurons (*P*-value = 0.2377, as compared to wild type). Rescue of *trx-1* expression in the intestine and ASI neurons did not restore proper SKN-1 nuclear localization (*P*-value < 0.0001 and *P*-value < 0.0001 as compared to wild type, respectively). (C) A schematic depicting the tissue localization of TRX-1 and SKN-1, emphasizing the absence of overlapping tissue expression between these two proteins. The ability of ASJ-expressed TRX-1 to regulate intestinal SKN-1 nuclear localization indicates a mechanism of cell non-autonomous regulation.

increased SKN-1::GFP nuclear localization threefold, as shown in Figure 1E. Restoring *trx-1* expression specifically in the ASJ neurons reduced SKN-1::GFP nuclear localization to levels seen in the *skn-1b/c::gfp* parent background. This suggests that TRX-1 regulates intestinal SKN-1::GFP nuclear accumulation cell non-autonomously from the ASJ neurons. To test whether intestinal SKN-1::GFP nuclear localization is inducible in the ASJ-specific complement of *trx-1*, the strain was exposed to oxidative stress. Intestinal SKN-1::GFP nuclear localization was partially restored (Figure S4). This finding further supports the observation that, when overexpressed, TRX-1 dampens the ability of oxidative stress to fully induce intestinal SKN-1::GFP nuclear localization (Figure S4). In contrast to the ASJ complement, restoring *trx-1* expression to the intestine or the ASI neurons did not rescue the SKN-1::GFP nuclear localization caused by loss of *trx-1*. It is interesting that artificially driving expression of *trx-1* in the intestine, the very same tissue in which SKN-1 localization is exhibited, could not restore proper SKN-1::GFP localization. This further suggests that a critical action required for TRX-1-dependent SKN-1 regulation must occur from the distal site of the ASJ neurons. Furthermore, while SKN-1::GFP is constitutively localized to the nuclei of the ASI neurons, expression of *trx-1* in these neurons does not abrogate SKN-1::GFP nuclear localization. This suggests that TRX-1 specifically affects intestinal SKN-1 protein.

The model in Figure 3C summarizes the expression pattern of both *trx-1* and *skn-1*. *skn-1* is expressed in both the ASI neurons and intestine. *trx-1* is expressed solely in the ASJ neurons. The cytoplasmic localization of SKN-1::GFP in the intestine occurs only when *trx-1* mutants are complemented with ASJ-specific *trx-1* expression. Therefore, we conclude that TRX-1 negatively impacts intestinal SKN-1 nuclear localization in a cell non-autonomous manner from the ASJ neurons.

TRX-1-dependent regulation of SKN-1 localization requires the p38 MAPK pathway

The p38 MAPK pathway is a critical regulator of SKN-1 localization and activation (Inoue *et al.* 2005). The p38 MAPK pathway is comprised of three kinases: NSY-1 (MAPKKK), SEK-1 (MAPKK), and PMK-1 (the p38 MAPK). One outcome of the stimulation of this pathway is the phosphorylation of SKN-1 at two serine residues, S74 and S340, leading to the nuclear translocation and transcriptional activation of this protein (Inoue *et al.* 2005). Highlighting the importance of this signaling pathway, in the absence of a functional p38 MAPK pathway or upon alanine substitution at these critical residues of SKN-1, intestinal SKN-1 nuclear localization and activation does not occur even during stress (Inoue *et al.* 2005). Given that TRX-1 negatively impacts intestinal SKN-1::GFP nuclear localization, we sought to address the dependence of this regulation on the p38 MAPK pathway.

First, we examined the importance of SKN-1 phosphorylation in mediating the TRX-1-dependent intestinal SKN-1 nuclear localization. To do this, we generated a *trx-1*; *skn-1(S74,340A)b/c::gfp* strain. While this strain did manifest higher background fluorescence in the intestine, the inability to phosphorylate SKN-1 at S74 and 340 resulted in cytoplasmic retention of SKN-1::GFP even upon loss of *trx-1* (Figure 4A), supported by the quantification of subcellular accumulation (Figure 4B). This suggests that TRX-1 functions to regulate SKN-1 nuclear translocation in a p38 phosphorylation-dependent manner. To further address the necessity of TRX-1-dependent SKN-1 regulation on the p38 MAPK pathway, we crossed the *trx-1*; *skn-1b/c::gfp* strain with null mutants of each p38 MAPK component [*nsy-1(ok593)*, *sek-1(km4)*, and *pmk-1(km25)*]. Fluorescent micrographs in Figure 4A and quantification in Figure 4B demonstrate that, while loss of *trx-1* alone causes a significant, threefold increase in intestinal SKN-1::GFP nuclear localization, compared to wild type, the additional loss of any component of the p38 MAPK significantly abrogates this phenotype. These data suggest that TRX-1-dependent regulation of intestinal SKN-1::GFP nuclear localization requires p38 MAPK-dependent phosphorylation of SKN-1 at serine residues 74 and 340.

Given that TRX-1-dependent regulation of intestinal SKN-1::GFP nuclear localization is dependent on the p38 MAPK pathway, we next assessed whether the dependence was direct or indirect, *i.e.*, in the same or a parallel pathway. One mechanism by which TRX-1 could modulate SKN-1::GFP localization in a direct, p38 MAPK-dependent manner would be to regulate the level of activity of a p38 MAPK component. To address this, we sought to determine whether *trx-1* mutants exhibit increased activation of NSY-1 and/or PMK-1, which was measured by assessing the levels of phosphorylation on the relevant residues in these kinases. In mammals, autophosphorylation of ASK1, the mammalian NSY-1 homolog, at Threonine 845 activates the kinase (Tobiume *et al.* 2002). In *C. elegans*, this threonine residue is found at position 829 of the amino acid sequence, and the surrounding amino acids are fully conserved between mammals and worms. We took advantage of a peptide-derived antibody specific for mammalian ASK1 phosphorylation at Threonine 845 that has previously been shown to cross-react with phosphorylated NSY-1 (Maruyama *et al.* 2014). To analyze PMK-1 activation, we obtained an antibody specific to PMK-1 phosphorylated at Threonine 180 and 182. (Schmeisser *et al.* 2013). Using Western blot analysis, we tested NSY-1 and PMK-1 phosphorylation in wild-type and *trx-1* mutants, which demonstrated no increase in active NSY-1 (Figure 4C) or active PMK-1 (Figure 4D) in a *trx-1* mutant, as compared to wild type. Exposure to sodium arsenite stress modestly increased NSY-1 activation and strongly increased PMK-1 phosphorylation, but to a similar extent in both wild type animals and *trx-1* mutants (Figure 4, C and D). It was previously demonstrated that *P. aeruginosa* infection increases NSY-1 phosphorylation dramatically (Maruyama *et al.* 2014). Similarly, we saw a dramatic increase in NSY-1 phosphorylation upon *P. aeruginosa* infection; however, the level of increased NSY-1 phosphorylation of *trx-1* mutants did not differ from that of wild-type animals (Figure S5). These data indicate that TRX-1 does not increase signaling through the p38 MAPK pathway, as measured by NSY-1 and PMK-1 phosphorylation levels, to cause the observed increase in SKN-1 nuclear localization. Overall, these experiments suggest that, while regulation of SKN-1 nuclear localization depends on p38 MAPK signaling, TRX-1 likely does not achieve this regulation by affecting the phosphorylation levels of the kinases.

TRX-1-dependent SKN-1 regulation does not result in the typical transcriptional activation of SKN-1 or an increase in any previously characterized protective responses

A classic hallmark of previously identified mechanisms of SKN-1 regulation is the correlation between intestinal SKN-1 nuclear localization and activation of the transcription factor, as exhibited by (i) resistance to both oxidative and pathogen stressors and (ii) the increased expression of phase II antioxidants (An and Blackwell 2003; An *et al.* 2005; Inoue *et al.* 2005; Tullet *et al.* 2008; Hoeven *et al.* 2011; Leung *et al.* 2014). Given that loss of *trx-1* dramatically increases intestinal SKN-1 nuclear localization, we predicted that *trx-1* mutants would exhibit increased expression of SKN-1-dependent antioxidants and demonstrate resistance to previously characterized oxidative and pathogen stressors (Wang *et al.* 1996; Oliveira *et al.* 2009; Hoeven *et al.* 2011). As previously shown with other oxidative stressors (Jee *et al.* 2005), *trx-1* mutants were mildly sensitive to 10 mM sodium arsenite (oxidative stress). (Figure 5A).

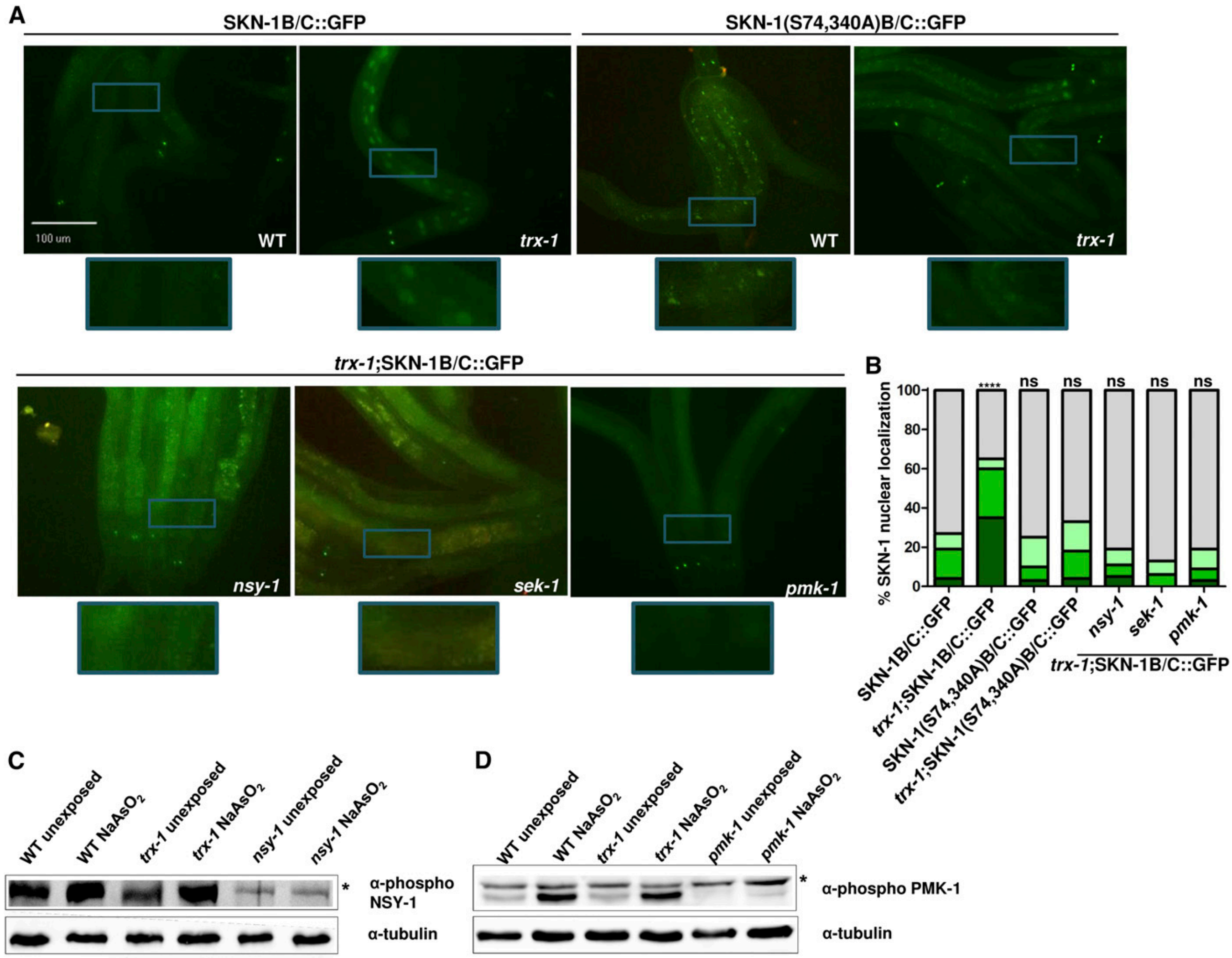

Figure 4 TRX-1-dependent regulation of SKN-1 nuclear localization is dependent on the p38 MAPK pathway. (A) Fluorescence microscopy was used to analyze *trx-1* worms that express a mutant form of SKN-1 [SKN-1(S74,340A)B/C::GFP], which cannot be phosphorylated by PMK-1. The increased percentage of intestinal SKN-1 nuclear localization seen upon loss of *trx-1* was abrogated upon mutation of Serines 74 and 340 of SKN-1. Mutants of p38 MAPK pathway components (*nsy-1*, *sek-1*, and *pmk-1*) were crossed into *trx-1*; *skn-1b/c::gfp* animals and viewed by fluorescence microscopy. The increased percentage of intestinal SKN-1 nuclear localization seen upon loss of *trx-1* was abrogated upon the additional loss of each p38 MAPK-signaling component. Wild-type and *trx-1* mutants with a *skn-1b/c::gfp* background are shown as controls. Worms were visualized using a 20× objective. Blue boxes indicate the portion of the micrograph field that is magnified in the boxes below each micrograph. (B) Percentage of SKN-1::GFP nuclear localization was categorically scored and quantified as described in *Materials and Methods*. Percentages are an average of three biological replicates ($n \geq 50$ worms per replicate). *trx-1* mutants expressing the mutated form of SKN-1 did not exhibit increased nuclear SKN-1 localization (*P*-value = 0.4895, as compared to wild type). *trx-1(ok1449)*; *nsy-1(ok593)*, *trx-1(ok1449)*; *sek-1(km4)* and *trx-1(ok1449)*; *pmk-1(km25)* mutants did not exhibit the increased SKN-1 localization seen in *trx-1* single mutants (*P*-value = 0.9629, *P*-value = 0.2322, and *P*-value = 0.8863, as compared to wild type, respectively). (C) Western blotting was used to analyze the level of phosphorylation (at residue Thr829) of NSY-1 in wild-type and *trx-1* mutants with and without exposure to the oxidative stressor sodium arsenite. NSY-1 phosphorylation was not increased in *trx-1* mutants, as compared to wild-type animals, regardless of sodium arsenite exposure. *nsy-1* mutants served as a negative control and α-tubulin as a loading control. (D) Western blotting was used to analyze the level of phosphorylation (at residues Thr180 and Thr182) of PMK-1 in wild-type and *trx-1* mutants with and without exposure to the oxidative stressor sodium arsenite. PMK-1 phosphorylation was not increased in *trx-1* mutants, as compared to wild-type animals, regardless of sodium arsenite exposure. *pmk-1* mutants served as a negative control and α-tubulin as a loading control. Black asterisks indicate nonspecific bands. Both of the blots shown are representative of three biological replicates.

However, this may be explained by the intrinsic short-lived phenotype of *trx-1* worms (Jee *et al.* 2005; Miranda-Vizuete *et al.* 2006). Furthermore, *trx-1* mutants exhibited no significant increase in survival upon *E. faecalis* (Figure 5B) or *P. aeruginosa* (Figure 5C) infection (pathogen stress), indicating that loss of *trx-1* does not impact previously characterized *skn-1*-dependent protective stress responses (An and Blackwell 2003; Hoeven *et al.* 2011).

Next, we examined the transcriptional activity of SKN-1 in wild-type and *trx-1* mutants under both stressed and unstressed conditions. As previously mentioned, increased intestinal SKN-1::GFP nuclear localization typically results in an enhancement of its transcriptional activity (An *et al.* 2005; Inoue *et al.* 2005; Tullet *et al.* 2008; Leung *et al.* 2014). A transcriptional *gst-4*::*gfp* reporter strain, which acts as a readout of SKN-1-dependent transcriptional activation (Park *et al.* 2009), was crossed with the *trx-1* mutant and analyzed via fluorescence microscopy. Loss of *trx-1* did not significantly increase *gst-4* expression, as determined by GFP fluorescence in intestinal cells under unstressed conditions (Figure 5D). Furthermore, upon exposure to sodium arsenite, induction of this reporter in the intestine of *trx-1* mutants was comparable to that of wild type (Figure 5D). To enable the examination of additional SKN-1-regulated genes in a quantitative manner, qRT-PCR was utilized. In agreement with the *gst-4*::*gfp* reporter strain, loss of *trx-1* did not significantly increase gene expression of any of the 10 SKN-1-dependent genes analyzed (Oliveira *et al.* 2009), as compared to wild-type worms, under unstressed conditions or after exposure to sodium arsenite (Figure 5E). Furthermore, there is no significant difference in SKN-1-dependent transcripts in *trx-1*; *skn-1b/c*::*gfp* worms, as compared to *skn-1b/c*::*gfp* animals (Figure 5F). These data suggest that, while intestinal nuclear localization of SKN-1 is increased, loss of *trx-1* may not affect the classical antioxidant transcriptional activity of SKN-1.

Transcriptome analysis reveals changes in cuticle components and lipid localization and transport upon loss of trx-1

Because TRX-1-dependent SKN-1 nuclear localization did not appear to activate expression of the SKN-1 regulon in a limited analysis (Figure 5, D and E), we utilized a more unbiased approach to identify SKN-1-regulated genes in a *trx-1* mutant background. Furthermore, we wanted to better understand how loss of *trx-1* impacts the transcriptome as a whole. We used RNA-Seq to look at global transcriptional changes in *trx-1* mutants as compared to wild-type worms with and without exposure to sodium arsenite. Interestingly, loss of *trx-1* results in a decrease in gene expression, with 75 (with stress) and 62 (without stress) genes being down-regulated, while only 3 genes are up-regulated regardless of stress (Figure 6A). Specifically, upon loss of *trx*-1, there is a significant enrichment in the down-regulation of genes encoding cuticle components and lipid localization and transport (Figure 6B). Furthermore, RNA-Seq also validated that the oxidative stress transcriptional response in *trx-1* animals does not greatly differ from that of wild-type animals (Figure 6C). While *trx-1* animals have an overall lower gene expression changes than wild-type animals, regardless of stress, the enrichment levels of glutathione transferase activity do not differ between stressed *trx-1* and wild-type animals (Table S1, Table S2, and Table S3). While thioredoxins are commonly regarded as general, cellular antioxidants, these data suggest that this is not the major role of TRX-1. The RNA-Seq results were validated using qRT-PCR to verify the changes in gene expression of 6 down-regulated and 3 up-regulated genes (Figure 6D). Overall, we conclude that loss of *trx-1* causes a general down-regulation of the expression of cuticle components and lipid localization and transport genes. Furthermore, the transcriptional oxidative stress response does not seem to be impaired in *trx-1* animals, as compared to wild-type animals.

Three genes, *lips-6*, *lips-11*, and *lbp-8*, are up-regulated upon loss of *trx-1*. Interestingly, these three genes are related to lipid metabolism as they encode two lipase-like proteins and one lipid-binding protein, respectively. We were interested in addressing whether SKN-1 was important for the up-regulation of these genes. Using qRT-PCR, we examined the fold change of these genes in *trx-1* animals, as compared to wild type, after knockdown of *skn-1* via RNAi. Only *lips-6* expression is significantly reduced after knockdown of *skn-1* (Figure 6E), although it is not a complete reduction, suggesting that, while SKN-1 has an effect, other factors may be involved in *lips-6* regulation.

Discussion

Here, we demonstrate a novel mechanism of SKN-1 regulation in which TRX-1 specifically regulates intestinal SKN-1 nuclear localization in a redox-independent, cell non-autonomous fashion from the ASJ neurons (Figure 1; Figure 2; Figure 3). This method of regulation requires the p38 MAPK pathway, although whether this dependence is direct or indirect requires further study (Figure 4). While TRX-1 regulates nuclear accumulation of intestinal SKN-1, it does not impact SKN-1 transcriptional activity or previously characterized SKN-1-dependent protective responses (Figure 5). RNA-Seq revealed that loss of *trx-1* impacts the expression of both cuticle components and lipid localization and transport genes, indicating that TRX-1 may directly influence these processes (Figure 6). Figure 7 depicts a schematic summary our findings.

The ability of TRX-1 to impact intestinal SKN-1 nuclear localization is not shared by all thioredoxins, as loss of TRX-2 and TRX-3 had no effect (Figure 1). TRX-2 is a component of the mitochondrial thioredoxin system in several tissues and is 54% similar and 32% identical to TRX-1 (Cacho-Valadez *et al.* 2012). TRX-3 is localized to the cytoplasm and nuclei of intestinal cells, is important for resistance to certain bacterial and fungal pathogens, and is 42% similar and 26% identical to TRX-1 (Jimenez-Hidalgo *et al.* 2014). Given the differences in cellular expression patterns and subcellular localization, it is not surprising that the regulation of intestinal SKN-1 nuclear localization is not common to the thioredoxin family as a whole. However, given that TRX-3 is localized to the same tissue as SKN-1, we were surprised to find that loss of *trx-3* does not affect intestinal SKN-1 nuclear localization. These data suggest that a critical step in TRX-1-dependent SKN-1 regulation occurs from the ASJ neurons specifically and/or that regions of sequence unique to *trx-1* may be critical for its ability to regulate SKN-1 nuclear localization.

Thioredoxins utilize a pair of conserved, redox reactive cysteine residues at their active site to fulfill a variety of

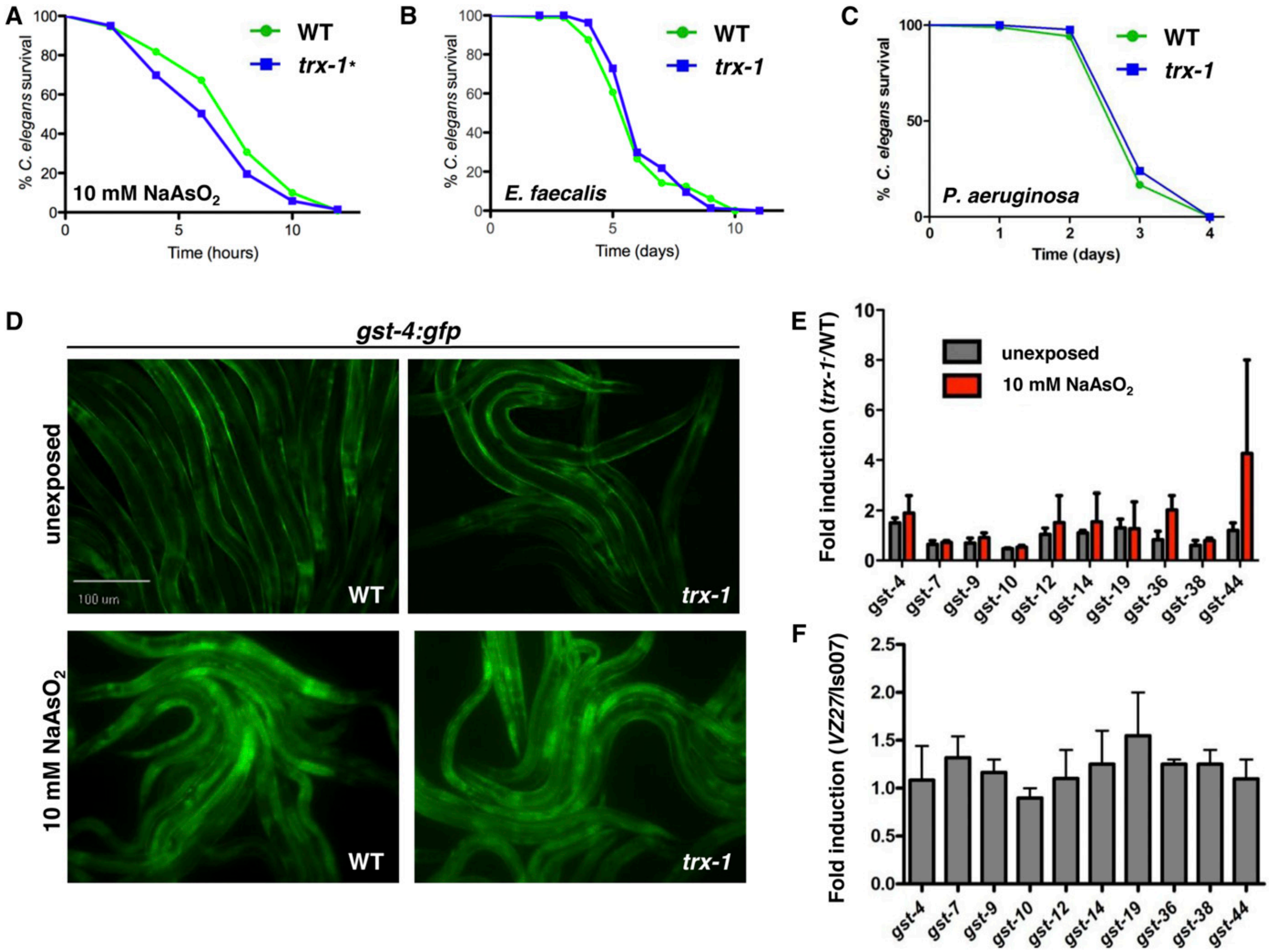

Figure 5 Loss of *trx-1* does not promote previously characterized SKN-1-dependent protective responses. (A–C) Resistance to several stressors, including (A) 10 mM sodium arsenite, (B) *E. faecalis* infection, and (C) *P. aeruginosa* infection was examined. *trx-1* mutants were mildly sensitive to oxidative stress induced by sodium arsenite (*P*-value = 0.02). Loss of *trx-1* did not significantly alter the ability to resist either pathogen infection (*P*-value = 0.3261 and *P*-value = 0.1527, respectively). (D) Fluorescence microscopy was used to analyze *gst-4*::*gfp* expression in wild-type and *trx-1* mutant animals with (bottom) and without (top) 5 hr of exposure to 10 mM sodium arsenite. *gst-4* expression was not induced in the intestine of *trx-1* mutants as compared to wild type. Worms were visualized using a 10× objective. (E) qRT-PCR was used to determine the fold change in SKN-1-dependent gene expression in *trx-1* mutants (as compared to wild-type animals) with (red bars) and without (black bars) 5 hr of exposure to 10 mM sodium arsenite. Expression of SKN-1-dependent genes did not significantly change in *trx-1* mutants, regardless of stress. (F) qRT-PCR was used to determine the fold change in SKN-1-dependent gene expression in *trx-1;skn-1b/c::gfp* (VZ27) animals as compared to *skn-1b/c::gfp* (Is007) control animals. The expression of SKN-1-dependent genes did not significantly change upon the loss of *trx-1* in the *skn-1b/c::gfp* parent background. The average gene expression of biological triplicates is shown, and the error bars represent SEM.

oxidoreductase-related functions, including maintenance of cellular homeostasis and regulation of transcription factors (reviewed in Holmgren 1985 and Holmgren and Lu 2010). However, thioredoxins also facilitate important cellular processes, such as chaperone-like functions, independently of their oxidoreductase functions (Du *et al.* 2015). Specifically in *C. elegans*, TRX-1 has been shown to modulate DAF-28 signaling during dauer formation in a redox-independent fashion (Fierro-Gonzalez *et al.* 2011a). "Redox dead" complementation of *trx-1* demonstrated that TRX-1 regulates SKN-1 in a manner independent of its redox status, expanding upon the list of redox-independent functions of TRX-1. This is further supported by the fact that there is no significant difference in the ability of stressed *trx-1* mutants, as compared to both stressed wild-type animals and unstressed *trx-1* mutants, to impact intestinal SKN-1 nuclear localization. These data suggest that TRX-1 negatively regulates intestinal SKN-1 nuclear localization regardless of its redox ability or the presence of an oxidative stressor.

Cell non-autonomous regulation is a classic method of coordinating an organism-wide response in a predictive, adaptive fashion. In *C. elegans*, cell non-autonomous signaling regulates several stress responses, including the heat-shock response, the unfolded protein response, pathogen stress response, and longevity (Prahlad *et al.* 2008; Sun *et al.* 2011; Taylor and Dillin 2013; Zhang *et al.* 2013; van

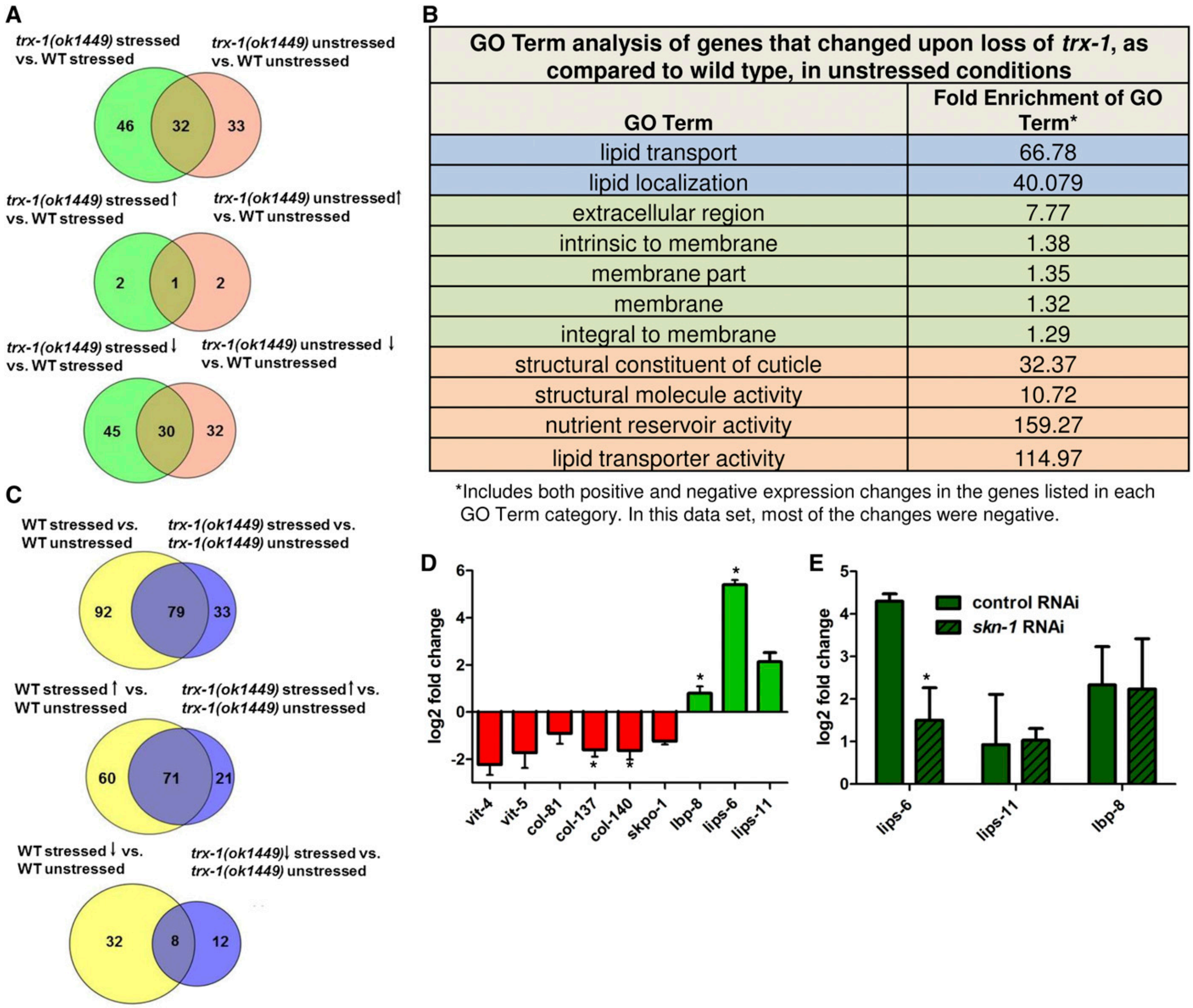

GO Term	Fold Enrichment of GO Term*
lipid transport	66.78
lipid localization	40.079
extracellular region	7.77
intrinsic to membrane	1.38
membrane part	1.35
membrane	1.32
integral to membrane	1.29
structural constituent of cuticle	32.37
structural molecule activity	10.72
nutrient reservoir activity	159.27
lipid transporter activity	114.97

Figure 6 Transcriptome analysis of *trx-1* mutants. (A) (Top) Number of shared genes significantly changed in *trx-1* animals, as compared to wild-type animals, under both stressed (10 mM sodium arsenite) and unstressed conditions. (Middle) Number of shared, overexpressed genes. (Bottom) Number of shared, underexpressed genes. (B) GO term analysis of genes that changed upon loss of *trx-1*, as compared to wild type, under unstressed conditions. Blue: biological processes; green: cellular component; orange: molecular function. (C) (Top) Number of shared genes significantly changed under stressed (10 mM sodium arsenite), as compared to unstressed, conditions in both wild-type and *trx-1* animals. (Middle) Number of shared, overexpressed genes. (Bottom) Number of shared, underexpressed genes. (D) qRT-PCR validation of select genes found to be differentially expressed using RNA-Seq upon loss of *trx-1*, as compared to wild type. The average gene expression of biological triplicates was graphed. Error bars represent the standard error of the mean (SEM), and an asterisk indicates a P-value < 0.05. (E) qRT-PCR was used to measure the $\log_2$-fold change in expression of the three up-regulated genes (*lips-6*, *lips-11*, *lbp-8*) upon loss of *trx-1*, as compared to wild type, after exposure to either *skn-1* RNAi or control RNAi. Expression of *lips-6* is partially dependent on *skn-1* (P-value = 0.032), while *lips-11* and *lbp-8* expression appears independent (P-value = 0.446 and P-value = 0.453, respectively). The average gene expression of biological triplicates was graphed, and error bars represent SEM.

Oosten-Hawle and Morimoto 2014a,b). In this work, we expand the list of stress pathways governed cell non-autonomously to include the oxidative stress transcription factor SKN-1. A variety of molecules, ranging from microRNAs to neurohormones and neuropeptides, signal between various tissues, including between the neurons and the intestine (van Oosten-Hawle and Morimoto 2014a,b). RNA-Seq of *trx-1* mutants revealed a change in gene expression of several lipid localization and transport genes. For example, *lbp-8*, an intestinal lipid chaperone that impacts two nuclear receptors, NHR-49 and NHR-80, to promote longevity (Folick, Oakley *et al.* 2015) was one of the genes with increased expression in the *trx-1* background. Lipids, such as yolk proteins, are implicated as signaling molecules (Grant and Hirsh 1999). Moreover, SKN-1 was recently implicated in the maintenance of lipid homeostasis. Specifically, certain lipids and the

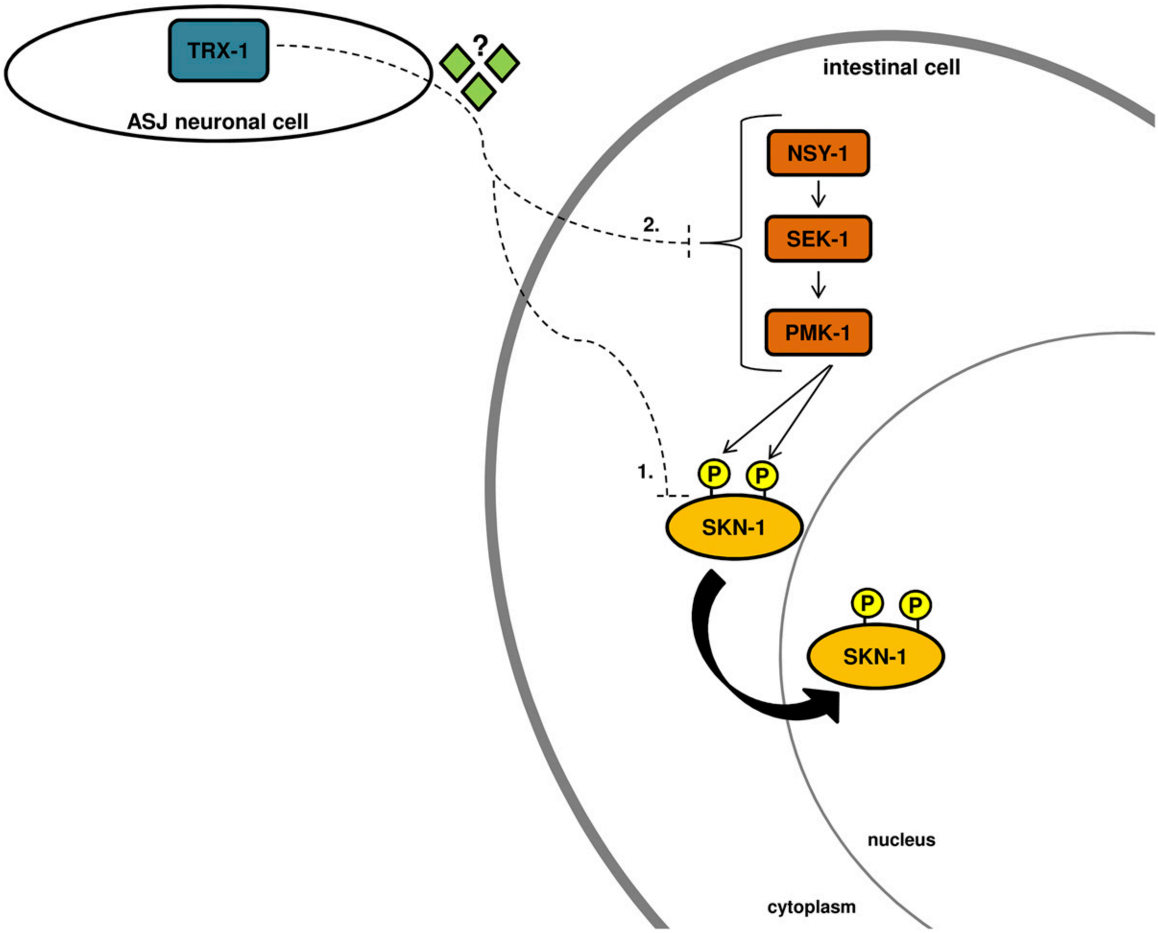

Figure 7 TRX-1 regulates SKN-1 nuclear localization cell non-autonomously. TRX-1 expressed in the ASJ neurons negatively controls nuclear localization of intestinal SKN-1, independently of its redox activity, probably through an unknown signaling intermediate. Two possible models by which ASJ-localized TRX-1 could cell non-autonomously direct SKN-1 nuclear localization in the intestine are shown. (1) A novel modification of SKN-1 could occur that results in p38 MAPK pathway-dependent nuclear localization of SKN-1, but not activation. (2) An alteration in signaling through the p38 MAPK pathway activity could cause SKN-1 localization without concurrent transcriptional activation.

activity of specific lipases were shown to activate SKN-1 in the absence of germline stem cells. In addition, SKN-1 was shown to regulate lipid metabolism in the absence of germline stem cells (Steinbaugh *et al.* 2015). In light of these recent findings and the work herein, we postulate that loss of *trx-1* affects intestinal SKN-1 nuclear localization via modulation of lipid homeostasis.

The requirement of the p38 MAPK pathway for TRX-1-dependent SKN-1 regulation was not surprising, given that the p38 MAPK-signaling pathway is essential in several previously identified mechanisms of SKN-1 regulation, including *daf-2*, *gsk-3*, and *wdr-23* (An *et al.* 2005; Tullet *et al.* 2008; Leung *et al.* 2014). Whether this is a direct or indirect dependence is still unknown, and several models can be postulated. First, it is possible that TRX-1 acts in the same pathway as p38 MAPK signaling to regulate SKN-1 localization. While we ruled out the possibility that loss of *trx-1* increases NSY-1 or PMK-1 phosphorylation, other post-translational modifications of either kinase may facilitate proper SKN-1 regulation in a TRX-1-dependent manner. Another possibility is that TRX-1 regulates intestinal SKN-1 nuclear localization in a pathway parallel to, but still dependent on, the p38 MAPK pathway. For example, TRX-1 may be able to regulate SKN-1 only after it has been phosphorylated by PMK-1 at serines 74 and 340 (Figure 7).

One of the more intriguing findings of this study was the severance of SKN-1 nuclear localization and transcriptional activation in the *trx-1* background. As previously mentioned, other mechanisms that affect nuclear localization of SKN-1 such as regulation via *gsk-3*, *wdr-23*, and the insulin and p38 MAPK-signaling pathways, are characterized by congruence between the degree of nuclear localization of intestinal SKN-1 and the degree of SKN-1-associated gene expression (An *et al.* 2005; Inoue *et al.* 2005; Tullet *et al.* 2008; Choe *et al.* 2009; Leung, Hasegawa *et al.* 2014). Dissociation of these phenotypes has been previously described, however. For example, several proteasome regulatory subunits and ubiquitin hydrolases result in increased intestinal SKN-1 nuclear localization but not increased *gst-4*. Furthermore, loss of certain chaperonins and a proteasomal protease, *pas-6*, elicits an opposite effect, in which increased *gst-4* expression does not result in detectable intestinal SKN-1 nuclear localization (Kahn *et al.* 2008). Additionally, loss of TOR signaling or treatment with rapamycin, which results in increased autophagy and decreased translation, causes an increase in SKN-1-associated gene expression without concomitant nuclear localization (Robida-Stubbs *et al.* 2012). In conclusion, TRX-1 is now one of several factors that affect intestinal SKN-1 nuclear localization in a manner independent of its degree of transcriptional activation. Understanding the basis of SKN-1 activity, or lack of activity, under these incongruous circumstances is an area ripe for future investigation.

Using RNA-Seq, we were able to look globally at the transcriptional impact of the loss of *trx-1*. This method was powerful for several reasons. First, it allowed us to verify that the SKN-1-dependent oxidative stress transcriptional response is not highly activated in *trx-1* animals. Additionally, the response to oxidative stress is unimpaired; it was activated in a relatively normal manner under oxidative stress conditions, as compared to wild-type animals (Table S1 and Table S2). Second, this approach allowed us to take an unbiased look at the classes of genes affected by the loss of *trx-1*. One prominent class of genes down-regulated upon loss of *trx-1* was the collagen gene family. Collagen is a critical structural component of the cuticle and the extracellular matrix (Page and Johnstone 2007). While no obvious cuticle defects are apparent in the *trx-1* mutant, it is possible that the structural integrity of the animals is affected. Furthermore, SKN-1-dependent collagen production is a key factor in maintaining a healthy extracellular matrix, ultimately promoting longevity (Ewald *et al.* 2014). This is of particular interest given that loss of *trx-1* results in a significant longevity defect (Jee *et al.* 2005; Miranda-Vizuete *et al.* 2006), which could potentially be explained by the down-regulation of collagen gene expression seen in this background. Finally, this approach allowed us to identify potential modulators of the TRX-1-dependent mechanism of intestinal SKN-1 nuclear localization. For example, the most enriched class of genes whose expression changes upon loss of *trx-1* are the lipid localization and transport genes. Interestingly, lipid gene regulators play a role in cell non-autonomous signaling in *C. elegans* (Zhang *et al.* 2013). Therefore, it is possible that TRX-1 present in the ASJ neurons uses its ability to modulate lipid localization and transport genes to affect intestinal SKN-1 nuclear localization cell non-autonomously.

In conclusion, we report that in *C. elegans* the major oxidative stress transcription factor, SKN-1, is cell non-autonomously regulated by the ASJ neurons via the thioredoxin TRX-1. This further expands the list of stress responses that are modulated from distant tissues at the organismal level. Additionally, we uncovered another example in which nuclear localization and activation of SKN-1 are not synonymous. Finally, the large number of collagen genes repressed in the *trx-1* mutant, based on our RNA-Seq data, may provide an explanation for why these animals are short-lived. While these findings increase the complexity of intestinal SKN-1 regulation, they highlight the importance of maintaining its proper regulation.

Acknowledgments

We thank T. K. Blackwell and the *Caenorhabditis* Genetics Center, which is funded by the National Institutes of Health (NIH) National Center for Research Resources, for the *C. elegans* strains. T. K. Blackwell is also acknowledged for sharing an aliquot of the FC4 antibody. We also thank V. Garcia and J. Hourihan for helpful advice regarding the use of phospho-specific antibodies for Western blotting. The research reported in this publication was supported by the National Institute of Allergy and Infectious Diseases and the National Institute of General Medical Sciences of the NIH under award nos. R01AI076406 (to D.A.G.) and R01GM98200 (to S.A.). S.A. was also supported by the American Cancer Society RSG014-044-DDC. A.M.-V. is a member of the EU-ROS (BM1203) and GENiE (BM1408) COST Actions, and his work was financed by grants from the Junta de Andalucía (Projects P07-CVI-02697 and P08-CVI-03629). P.S. was supported by the Swedish Research Council, the Torsten Söderberg and Åhlén Foundations, and by the Karolinska Institute Strategic Neurosciences Program. The content is solely the responsibility of the authors and does not necessarily represent the official views of the granting agencies.

Literature Cited

An, J. H., and T. K. Blackwell, 2003 SKN-1 links C. elegans mesendodermal specification to a conserved oxidative stress response. Genes Dev. 17: 1882–1893.

An, J. H., K. Vranas, M. Lucke, H. Inoue, N. Hisamoto *et al.*, 2005 Regulation of the Caenorhabditis elegans oxidative stress defense protein SKN-1 by glycogen synthase kinase-3. Proc. Natl. Acad. Sci. USA 102: 16275–16280.

Anderson, M. E., 1998 Glutathione: an overview of biosynthesis and modulation. Chem. Biol. Interact. 111–112: 1–14.

Arnér, E. S., and A. Holmgren, 2000 Physiological functions of thioredoxin and thioredoxin reductase. Eur. J. Biochem. 267: 6102–6109.

Berndt, C., C. H. Lillig, and A. Holmgren, 2008 Thioredoxins and glutaredoxins as facilitators of protein folding. Biochim. Biophys. Acta 1783: 641–650.

Bowerman, B., B. W. Draper, C. C. Mello, and J. R. Priess, 1993 The maternal gene skn-1 encodes a protein that is distributed unequally in early C. elegans embryos. Cell 74: 443–452.

Buchanan, B. B., A. Holmgren, J. P. Jacquot, and R. Scheibe, 2012 Fifty years in the thioredoxin field and a bountiful harvest. Biochim. Biophys. Acta 1820: 1822–1829.

Cacho-Valadez, B., F. Muñoz-Lobato, J. R. Pedrajas, J. Cabello, J. C. Fierro-González *et al.*, 2012 The characterization of the Caenorhabditis elegans mitochondrial thioredoxin system uncovers an unexpected protective role of thioredoxin reductase 2 in β-amyloid peptide toxicity. Antioxid. Redox Signal. 16: 1384–1400.

Carroll, B. T., G. R. Dubyak, M. M. Sedensky, and P. G. Morgan, 2006 Sulfated signal from ASJ sensory neurons modulates stomatin-dependent coordination in Caenorhabditis elegans. J. Biol. Chem. 281: 35989–35996.

Chávez, V., A. Mohri-Shiomi, and D. A. Garsin, 2009 Ce-Duox1/BLI-3 generates reactive oxygen species as a protective innate immune mechanism in Caenorhabditis elegans. Infect. Immun. 77: 4983–4989.

Choe, K. P., A. J. Przybysz, and K. Strange, 2009 The WD40 repeat protein WDR-23 functions with the CUL4/DDB1 ubiquitin ligase to regulate nuclear abundance and activity of SKN-1 in Caenorhabditis elegans. Mol. Cell. Biol. 29: 2704–2715.

Du, H., S. Kim, Y. S. Hur, M. S. Lee, S. H. Lee *et al.*, 2015 A cytosolic thioredoxin acts as a molecular chaperone for peroxisome matrix proteins as well as antioxidant in peroxisome. Mol. Cells 38: 187–194.

Edgar, L. G., and J. D. McGhee, 1986 Embryonic expression of a gut-specific esterase in Caenorhabditis elegans. Dev. Biol. 114: 109–118.

Ewald, C. Y., J. N. Landis, J. P. Abate, C. T. Murphy, and T. K. Blackwell, 2014 Dauer-independent insulin/IGF-1-signalling implicates collagen remodelling in longevity. Nature 519: 97–101.

Fierro-González, J. C., A. Cornils, J. Alcedo, A. Miranda-Vizuete, and P. Swoboda, 2011a The thioredoxin TRX-1 modulates the function of the insulin-like neuropeptide DAF-28 during dauer formation in Caenorhabditis elegans. PLoS One 6: e16561.

Fierro-González, J. C., M. González-Barrios, A. Miranda-Vizuete, and P. Swoboda, 2011b The thioredoxin TRX-1 regulates adult lifespan extension induced by dietary restriction in Caenorhabditis elegans. Biochem. Biophys. Res. Commun. 406: 478–482.

Folick, A., H. D. Oakley, Y. Yu, E. H. Armstrong, M. Kumari *et al.*, 2015 Aging. Lysosomal signaling molecules regulate longevity in Caenorhabditis elegans. Science 347: 83–86.

Fujino, G., T. Noguchi, K. Takeda, and H. Ichijo, 2006 Thioredoxin and protein kinases in redox signaling. Semin. Cancer Biol. 16: 427–435.

Fujino, G., T. Noguchi, A. Matsuzawa, S. Yamauchi, M. Saitoh *et al.*, 2007 Thioredoxin and TRAF family proteins regulate reactive oxygen species-dependent activation of ASK1 through reciprocal modulation of the N-terminal homophilic interaction of ASK1. Mol. Cell. Biol. 27: 8152–8163.

Garsin, D. A., C. D. Sifri, E. Mylonakis, X. Qin, K. V. Singh *et al.*, 2001 A simple model host for identifying Gram-positive virulence factors. Proc. Natl. Acad. Sci. USA 98: 10892–10897.

Glover-Cutter, K. M., S. Lin, and T. K. Blackwell, 2013 Integration of the unfolded protein and oxidative stress responses through SKN-1/Nrf. PLoS Genet. 9: e1003701.

González-Barrios, M., J. C. Fierro-González, E. Krpelanova, J. A. Mora-Lorca, J. R. Pedrajas *et al.*, 2015 *Cis*- and *trans*-regulatory mechanisms of gene expression in the ASJ sensory neuron of *Caenorhbditis elegans*. Genetics 200: 123–134.

Grant, B., and D. Hirsh, 1999 Receptor-mediated endocytosis in the Caenorhabditis elegans oocyte. Mol. Biol. Cell 10: 4311–4326.

Hoeven, Rv., K. C. McCallum, M. R. Cruz, and D. A. Garsin, 2011 Ce-Duox1/BLI-3 generated reactive oxygen species trigger protective SKN-1 activity via p38 MAPK signaling during infection in C. elegans. PLoS Pathog. 7: e1002453.

Holmgren, A., 1985 Thioredoxin. Annu. Rev. Biochem. 54: 237–271.

Holmgren, A., and J. Lu, 2010 Thioredoxin and thioredoxin reductase: current research with special reference to human disease. Biochem. Biophys. Res. Commun. 396: 120–124.

Hope, I. A., 1999 *C. elegans: A Practical Approach*. The Practical Approach Series, Oxford University Press, Oxford.

Huang da, W., B. T. Sherman, and R. A. Lempicki, 2009a Bioinformatics enrichment tools: paths toward the comprehensive functional analysis of large gene lists. Nucleic Acids Res. 37: 1–13.

Huang da, W., B. T. Sherman, and R. A. Lempicki, 2009b Systematic and integrative analysis of large gene lists using DAVID bioinformatics resources. Nat. Protoc. 4: 44–57.

Hybertson, B. M., B. Gao, S. K. Bose, and J. M. McCord, 2011 Oxidative stress in health and disease: the therapeutic potential of Nrf2 activation. Mol. Aspects Med. 32: 234–246.

Inoue, H., N. Hisamoto, J. H. An, R. P. Oliveira, E. Nishida *et al.*, 2005 The C. elegans p38 MAPK pathway regulates nuclear localization of the transcription factor SKN-1 in oxidative stress response. Genes Dev. 19: 2278–2283.

Jee, C., L. Vanoaica, J. Lee, B. J. Park, and J. Ahnn, 2005 Thioredoxin is related to life span regulation and oxidative stress response in Caenorhabditis elegans. Genes Cells 10: 1203–1210.

Jiménez-Hidalgo, M., C. L. Kurz, J. R. Pedrajas, F. J. Naranjo-Galindo, M. González-Barrios *et al.*, 2014 Functional characterization of thioredoxin 3 (TRX-3), a Caenorhabditis elegans intestine-specific thioredoxin. Free Radic. Biol. Med. 68: 205–219.

Kahn, N. W., S. L. Rea, S. Moyle, A. Kell, and T. E. Johnson, 2008 Proteasomal dysfunction activates the transcription factor SKN-1 and produces a selective oxidative-stress response in Caenorhabditis elegans. Biochem. J. 409: 205–213.

Langmead, B., C. Trapnell, M. Pop, and S. L. Salzberg, 2009 Ultrafast and memory-efficient alignment of short DNA sequences to the human genome. Genome Biol. 10: R25.

Leung, C. K., K. Hasegawa, Y. Wang, A. Deonarine, L. Tang *et al.*, 2014 Direct interaction between the WD40 repeat protein WDR-23 and SKN-1/Nrf inhibits binding to target DNA. Mol. Cell. Biol. 34: 3156–3167.

Liu, Y., and W. Min, 2002 Thioredoxin promotes ASK1 ubiquitination and degradation to inhibit ASK1-mediated apoptosis in a redox activity-independent manner. Circ. Res. 90: 1259–1266.

Loria, P. M., J. Hodgkin, and O. Hobert, 2004 A conserved postsynaptic transmembrane protein affecting neuromuscular signaling in Caenorhabditis elegans. J. Neurosci. 24: 2191–2201.

Lushchak, V. I., 2011 Adaptive response to oxidative stress: bacteria, fungi, plants and animals. Comp. Biochem. Physiol. C Toxicol. Pharmacol. 153: 175–190.

Lynn, D. A., H. M. Dalton, J. N. Sowa, M. C. Wang, A. A. Soukas *et al.*, 2015 Omega-3 and -6 fatty acids allocate somatic and germline lipids to ensure fitness during nutrient and oxidative stress in Caenorhabditis elegans. Proc. Natl. Acad. Sci. USA 112: 15378–15383.

Mahajan-Miklos, S., M. W. Tan, L. G. Rahme, and F. M. Ausubel, 1999 Molecular mechanisms of bacterial virulence elucidated using a Pseudomonas aeruginosa-Caenorhabditis elegans pathogenesis model. Cell 96: 47–56.

Marinho, H. S., C. Real, L. Cyrne, H. Soares, and F. Antunes, 2014 Hydrogen peroxide sensing, signaling and regulation of transcription factors. Redox Biol. 2: 535–562.

Maruyama, T., T. Araki, Y. Kawarazaki, I. Naguro, S. Heynen *et al.*, 2014 Roquin-2 promotes ubiquitin-mediated degradation of ASK1 to regulate stress responses. Sci. Signal. 7: ra8.

McCord, J. M., and I. Fridovich, 1969 Superoxide dismutase. An enzymic function for erythrocuprein (hemocuprein). J. Biol. Chem. 244: 6049–6055.

Miranda-Vizuete, A., J. C. Fierro González, G. Gahmon, J. Burghoorn, P. Navas *et al.*, 2006 Lifespan decrease in a Caenorhabditis elegans mutant lacking TRX-1, a thioredoxin expressed in ASJ sensory neurons. FEBS Lett. 580: 484–490.

Oliveira, R. P., J. Porter Abate, K. Dilks, J. Landis, J. Ashraf *et al.*, 2009 Condition-adapted stress and longevity gene regulation by Caenorhabditis elegans SKN-1/Nrf. Aging Cell 8: 524–541.

Page, A. P., and I. L. Johnstone, 2007 The cuticle. (March 19, 2007), WormBook, ed. The C. elegans Research Community, WormBook, doi/10.1895/wormbook.1.138.1, http://www.wormbook.org.

Park, S. K., P. M. Tedesco, and T. E. Johnson, 2009 Oxidative stress and longevity in Caenorhabditis elegans as mediated by SKN-1. Aging Cell 8: 258–269.

Powis, G., and W. R. Montfort, 2001 Properties and biological activities of thioredoxins. Annu. Rev. Biophys. Biomol. Struct. 30: 421–455.

Prahlad, V., T. Cornelius, and R. I. Morimoto, 2008 Regulation of the cellular heat shock response in Caenorhabditis elegans by thermosensory neurons. Science 320: 811–814.

Ray, P. D., B. W. Huang, and Y. Tsuji, 2012 Reactive oxygen species (ROS) homeostasis and redox regulation in cellular signaling. Cell. Signal. 24: 981–990.

Robida-Stubbs, S., K. Glover-Cutter, D. W. Lamming, M. Mizunuma, S. D. Narasimhan *et al.*, 2012 TOR signaling and rapamycin influence longevity by regulating SKN-1/Nrf and DAF-16/FoxO. Cell Metab. 15: 713–724.

Salazar, M., A. I. Rojo, D. Velasco, R. M. de Sagarra, and A. Cuadrado, 2006 Glycogen synthase kinase-3beta inhibits the xenobiotic and antioxidant cell response by direct phosphorylation and nuclear exclusion of the transcription factor Nrf2. J. Biol. Chem. 281: 14841–14851.

Schackwitz, W. S., T. Inoue, and J. H. Thomas, 1996 Chemosensory neurons function in parallel to mediate a pheromone response in C. elegans. Neuron 17: 719–728.

Schmeisser, S., S. Priebe, M. Groth, S. Monajembashi, P. Hemmerich *et al.*, 2013 Neuronal ROS signaling rather than AMPK/sirtuin-mediated energy sensing links dietary restriction to lifespan extension. Mol. Metab. 2: 92–102.

Steinbaugh, M. J., S. D. Narasimhan, S. Robida-Stubbs, L. E. Moronetti Mazzeo, J. M. Dreyfuss *et al.*, 2015 Lipid-mediated regulation of SKN-1/Nrf in response to germ cell absence. eLife 4: 4.

Sun, J., V. Singh, R. Kajino-Sakamoto, and A. Aballay, 2011 Neuronal GPCR controls innate immunity by regulating noncanonical unfolded protein response genes. Science 332: 729–732.

Taylor, R. C., and A. Dillin, 2013 XBP-1 is a cell-nonautonomous regulator of stress resistance and longevity. Cell 153: 1435–1447.

Thanan, R., S. Oikawa, Y. Hiraku, S. Ohnishi, N. Ma *et al.*, 2014 Oxidative stress and its significant roles in neurodegenerative diseases and cancer. Int. J. Mol. Sci. 16: 193–217.

Tobiume, K., M. Saitoh, and H. Ichijo, 2002 Activation of apoptosis signal-regulating kinase 1 by the stress-induced activating phosphorylation of pre-formed oligomer. J. Cell. Physiol. 191: 95–104.

Trapnell, C., A. Roberts, L. Goff, G. Pertea, D. Kim *et al.*, 2012 Differential gene and transcript expression analysis of RNA-seq experiments with TopHat and Cufflinks. Nat. Protoc. 7: 562–578.

Trapnell, C., D. G. Hendrickson, M. Sauvageau, L. Goff, J. L. Rinn *et al.*, 2013 Differential analysis of gene regulation at transcript resolution with RNA-seq. Nat. Biotechnol. 31: 46–53.

Tullet, J. M., M. Hertweck, J. H. An, J. Baker, J. Y. Hwang *et al.*, 2008 Direct inhibition of the longevity-promoting factor SKN-1 by insulin-like signaling in C. elegans. Cell 132: 1025–1038.

van Oosten-Hawle, P., and R. I. Morimoto, 2014a Organismal proteostasis: role of cell-nonautonomous regulation and transcellular chaperone signaling. Genes Dev. 28: 1533–1543.

van Oosten-Hawle, P., and R. I. Morimoto, 2014b Transcellular chaperone signaling: an organismal strategy for integrated cell stress responses. J. Exp. Biol. 217: 129–136.

Walker, A. K., R. See, C. Batchelder, T. Kophengnavong, J. T. Gronniger *et al.*, 2000 A conserved transcription motif suggesting functional parallels between Caenorhabditis elegans SKN-1 and Cap'n'Collar-related basic leucine zipper proteins. J. Biol. Chem. 275: 22166–22171.

Wang, T. S., C. F. Kuo, K. Y. Jan, and H. Huang, 1996 Arsenite induces apoptosis in Chinese hamster ovary cells by generation of reactive oxygen species. J. Cell. Physiol. 169: 256–268.

Yoshioka, J., E. R. Schreiter, and R. T. Lee, 2006 Role of thioredoxin in cell growth through interactions with signaling molecules. Antioxid. Redox Signal. 8: 2143–2151.

Zhang, P., M. Judy, S. J. Lee, and C. Kenyon, 2013 Direct and indirect gene regulation by a life-extending FOXO protein in C. elegans: roles for GATA factors and lipid gene regulators. Cell Metab. 17: 85–100.

Communicating editor: M. V. Sundaram

GENETICS

Supporting Information
www.genetics.org/lookup/suppl/doi:10.1534/genetics.115.185272/-/DC1

TRX-1 Regulates SKN-1 Nuclear Localization Cell Non-autonomously in *Caenorhabditis elegans*

Katie C. McCallum, Bin Liu, Juan Carlos Fierro-González, Peter Swoboda, Swathi Arur, Antonio Miranda-Vizuete, and Danielle A. Garsin

DOI: 10.1534/genetics.115.185272

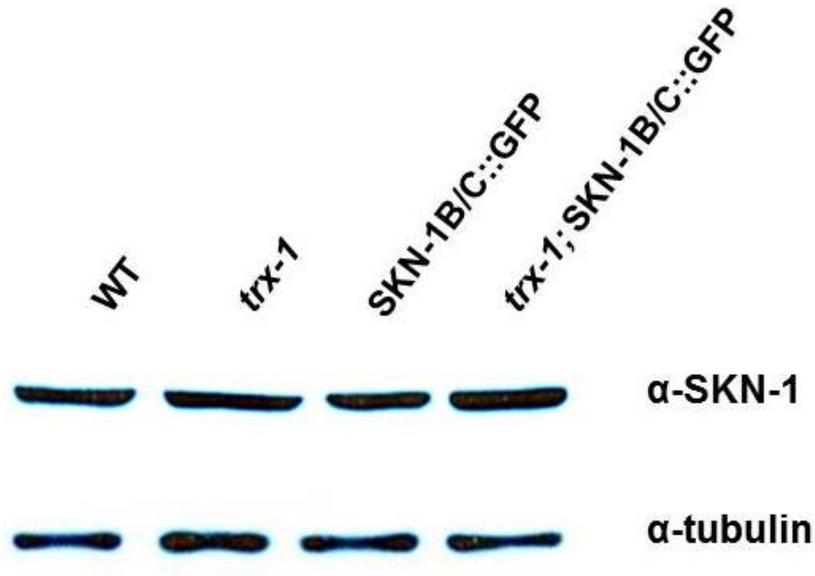

Figure S1. SKN-1 protein levels remain unchanged in *trx-1* mutants. Western blotting was used to analyze endogenous SKN-1C protein levels in wild type, *trx-1*, *skn-1b/c::gfp*, and *trx-1*; *skn-1b/c::gfp* worms. SKN-1C protein levels remain unchanged upon loss of *trx-1* in both the wild type and *skn-1b/c::gfp* backgrounds. α-tubulin served as a loading control.

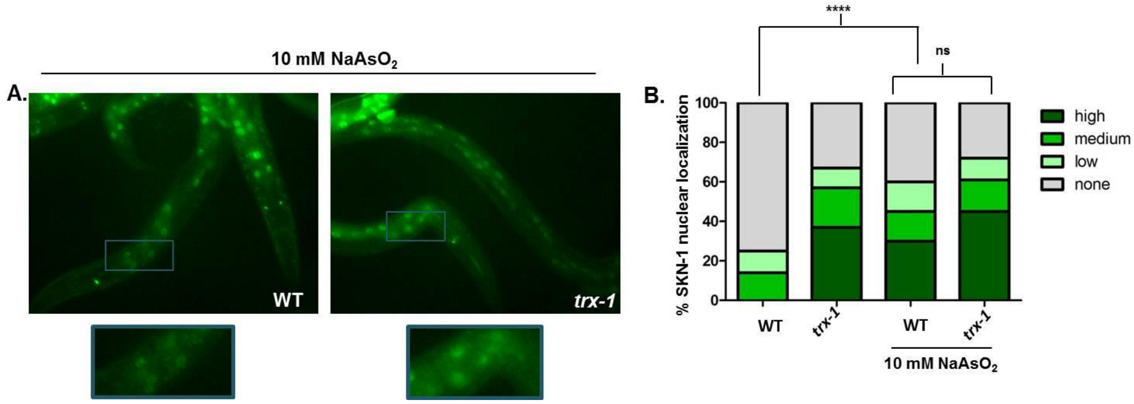

Figure S2. Intestinal SKN-1 nuclear localization is increased as a result of exposure to Sodium Arsenite and it is not further increased upon *trx-1* loss*.* A) Fluorescence microscopy was used to analyze the intestinal nuclear localization of SKN-1 (SKN-1B/C::GFP) in wild type and *trx-1* worms after being exposed to 10mM $NaAsO_2$ for three hours at 20°C. Worms were visualized using a 20X objective. Blue boxes indicate the portion of the micrograph field that is magnified in the boxes below each micrograph. Control animals not exposed to NaAsO2 are shown in Figure 1A and B. **B)** Percent SKN-1 nuclear localization was categorically scored and quantified as described in Materials and Methods. Intestinal SKN-1 nuclear localization significantly increased during oxidative stress (*P*-value < 0.0001). The degree to which intestinal SKN-1 nuclear localization increases upon loss of *trx-1* is similar to that seen upon exposure to the oxidative stressor, sodium arsenite (*P*-value 0.64, as compared to wild type) and their effects on SKN-1 nuclear localization are not additive.

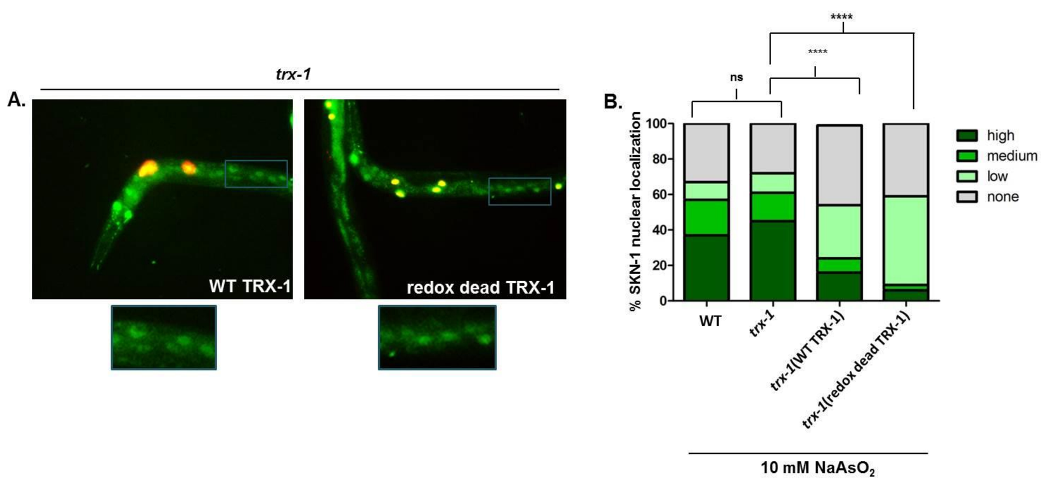

Figure S3. Intestinal SKN-1 nuclear localization upon both wild type and redox dead *trx-1* complementation is increased upon exposure to Sodium Arsenite. A) Fluorescence microscopy was used to analyze the intestinal nuclear localization of SKN-1 (SKN-1B/C::GFP) upon complementation of wild type or 'redox dead' *trx-1* after being exposed to 10mM $NaAsO_2$ for three hours at 20°C. Worms were visualized using a 20X objective. Blue boxes indicate the portion of the micrograph field that is magnified in the boxes below each micrograph. Non-transgenic controls can be seen in Supplementary Figure 2A. **B)** Percent SKN-1 nuclear localization was categorically scored and quantified as described in Materials and Methods. Both wild type and 'redox dead' complement of *trx-1* partially restored proper intestinal SKN-1 nuclear localization upon exposure to oxidative stress (*P*-value < 0.0001 and *P*-value < 0.0001, respectively, as compared to *trx-1*; *skn-1b/c::gfp*), indicating that intestinal SKN-1 nuclear localization is indeed inducible in this strain, however the ability to properly promote SKN-1 localization during stress is dampened by the overexpression of *trx-1*.

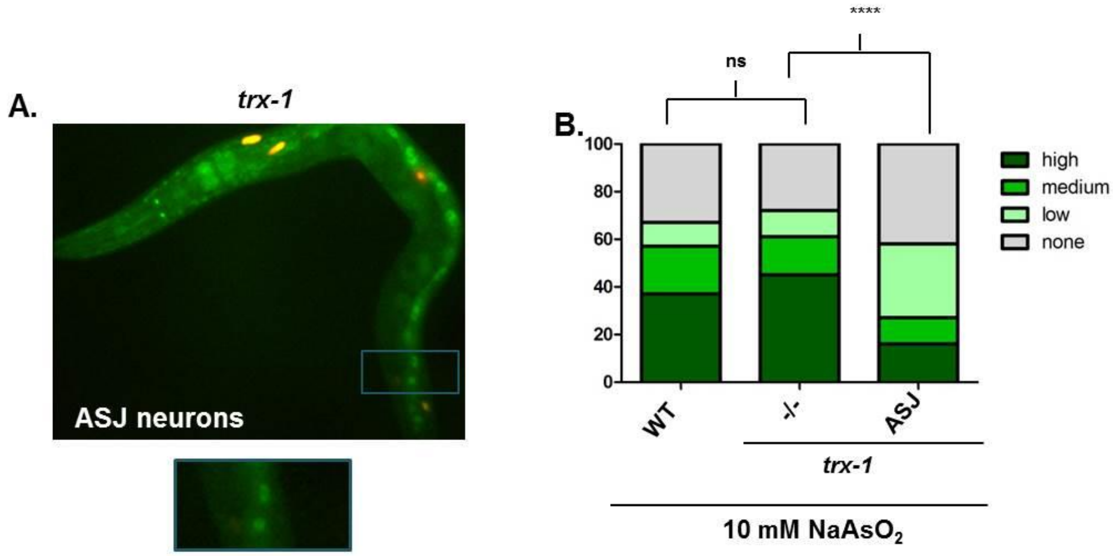

Figure S4. Intestinal SKN-1 nuclear localization upon ASJ-specific rescue of *trx-1* is increased upon exposure to Sodium Arsenite. A) Fluorescence microscopy was used to analyze the intestinal nuclear localization of SKN-1 (SKN-1B/C::GFP) upon rescue of *trx-1* animals with ASJ-specific expression of wild type *trx-1* after being exposed to 10mM $NaAsO_2$ for three hours at 20°C. Worms were visualized using a 20X objective. Blue boxes indicate the portion of the micrograph field that is magnified in the boxes below each micrograph. Non-transgenic controls can be seen in Supplementary Figure 1A. **B)** Percent SKN-1 nuclear localization was categorically scored and quantified as described in Materials and Methods. ASJ-specific rescue of *trx-1* resulted in partial intestinal SKN-1 nuclear localization upon exposure to oxidative stress; a statistically significant difference of *P*-value < 0.0001, was apparent when the ASJ complement was compared to the parent background of *trx-1*; *skn-1b/c::gfp*.

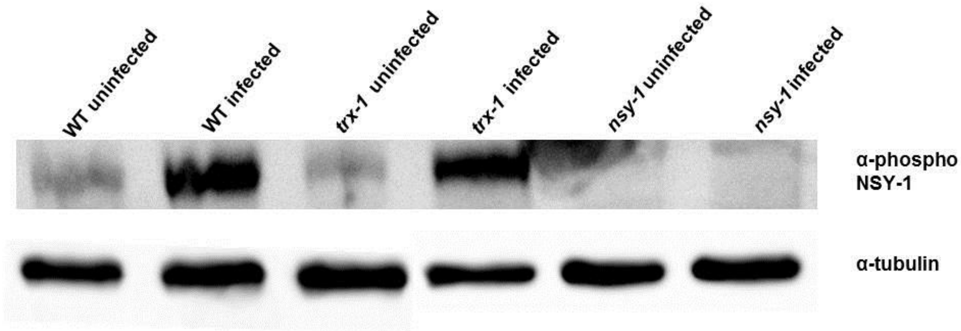

Figure S5. *Pseudomonas aeruginosa* infection increases NSY-1 phosphorylation to a similar extent in both wild type animals and *trx-1* mutants.
Western blotting was used to analyze the level of phosphorylation (at residue Thr829) of NSY-1 in wild type and *trx-1* mutants after being infected with *Pseudomonas aeruginosa* (as compared to uninfected worms) for 3 hours. NSY-1 phosphorylation was increased upon infection, however this increase did not differ between *trx-1* mutants and wild type animals. *nsy-1* mutants served as a negative control and α-tubulin as a loading control.

Table S1. GO Term analysis of *trx-1* mutants with and without stress.
Oxidative stress response genes are enriched upon 5 hours of 10mM sodium arsenite oxidative stress.

***trx-1* (ok1449) stressed vs. unstresssed**			
Category	**Term**	**Count**	**Fold Enrichment**
BP	Response to heat	4	35.4
BP	Determination of adult lifespan	7	7.1
BP	Aging	7	6.8
BP	Multicellular organismal aging	7	6.8
BP	Response to abiotic stimulus	5	13.5
BP	Oxidation reduction	8	5.0
MF	Catalytic activity	36	1.92
MF	Glutathione transferase activity	5	58.0
MF	Oxidoreductase activity	13	4.5
MF	Transferase activity, transferring alkyl or aryl (other than methyl) groups	5	28.1

Table S2. GO Term analysis of stressed *trx-1* mutants, as compared to wild type. Genes that encode components of the cuticle are also enriched upon loss of *trx-1* during stress.

***trx-1* (ok1449) vs. WT (stressed)**			
Category	**Term**	**Count**	**Fold Enrichment**
BP	Developmental process	21	1.8
CC	Membrane	35	1.3
CC	Membrane part	34	1.3
MF	Structural constituent of cuticle	24	36.0
MF	Structural molecule activity	25	13.0

Table S3. GO Term analysis of wild type animals with and without stress. Oxidative stress response genes are enriched upon 5 hours of 10mM sodium arsenite oxidative stress.

WT stressed vs. unstressed			
Category	**Term**	**Count**	**Fold Enrichment**
BP	Aging	13	8.7
BP	Determination of adult lifespan	13	8.7
BP	Multicellular organismal aging	13	8.7
BP	Response to temperature stimulus	6	22.0
BP	Lipid transport	5	34.0
BP	ER-nuclear signaling pathway	4	71.0
BP	ER unfolded protein response	4	71.0
BP	Response to heat	5	30.0
BP	Response to ER stress	4	65.0
BP	Cellular response to unfolded protein	4	59.0
BP	Response to stress	10	5.4
BP	Response to unfolded protein	4	50.0
BP	Response to protein stimulus	4	50.0
BP	Lipid localization	5	20.0
BP	Response to abiotic stimulus	6	11.0
BP	Response to biotic stimulus	4	30.0
BP	Cellular response to stress	6	9.2
BP	Response to organic substance	4	23.0
BP	Cellular response to stimulus	6	7.6
MF	Nutrient reservoir activity	5	115.0
MF	Glutathione transferase activity	5	41.0
MF	Lipid transport activity	5	39.0
MF	Catalytic activity	45	1.7
MF	Transferase activity. Transferring alkyl or aryl (other than methyl) groups	5	20.0
MF	Oxidoreductase activity	14	3.3

Table S4. Strains used in this study.

Strain Name	Genotype	Reference
N2	Wild type Bristol	
VZ1	*trx-1(ok1449) II*	[1]
CL2166	*dvIs19 [Pgst-4::gfp::NLS; rol-6(su1006)] III*	[2]
LD007	*Is007 [skn-1b/c::gfp; rol-6(su1006)] X*	[3]
LD1782	*Ex060 [skn-1(S74,340A)b/c::gfp; rol-6(su1006)]*	[4]
OE4064	*trx-1(ok1449) II; daf-28(sa191) V; ofEx416 [Ptrx-1::trx-1::gfp; Punc-122::DsRed]*	[5]
OE4067	*trx-1(ok1449) II; daf-28(sa191) V; ofEx419 [Ptrx-1::trx-1(SGPS)::gfp; Punc-122::DsRed]*	[5]
VC390	*nsy-1(ok593) II*	CGC
KU4	*sek-1(km4) X*	CGC
KU25	*pmk-1(km25) IV*	CGC
OE3381	*lin-15(n765ts) X ; ofEx284 [Ptrx-1::trx-1::gfp::trx-1 3´-UTR; lin-15ab (+)]*	This study
VZ27	*trx-1(ok1449) II; Is007 [skn-1b/c::gfp; rol-6(su1006)] X*	This study
VZ26	*trx-2(tm2720) V*; *Is007 [skn-1b/c::gfp; rol-6(su1006)] X*	This study
VZ157	*trx-3(tm2820) IV* ; *Is007 [skn-1b/c::gfp; rol-6(su1006)] X*	This study
VZ472	*trx-1(ok1449) II; vzEx168 [Pssu-1::trx-1::trx-1 3´-UTR; Punc-122::DsRed]*	This study
VZ458	*vzEx163 [Pges-1::trx-1::trx-1 3'-UTR; Punc-122::DsRed]*	This study
VZ461	*vzEx166 [Pdaf-7::trx-1::trx-1 3'-UTR; Punc-122::DsRed]*	This study
VZ433	*trx-1(ok1449) II*; *dvIs19 [Pgst-4::gfp::NLS; rol-6(su1006)] III*	This study
GF92	*trx-1(ok1449) II; Is007 [skn-1b/c::gfp; rol-6(su1006)] X; vzEx168 [Pssu-1::trx-1::trx-1 3´-UTR; Punc-122::DsRed]*	This study
GF93	*trx-1(ok1449) II; Is007 [skn-1b/c::gfp; rol-6(su1006)] X; vzEx163 [Pges-1::trx-1::trx-1 3'-UTR; Punc-122::DsRed]*	This study
GF94	*trx-1(ok1449) II; Is007 [skn-1b/c::gfp; rol-6(su1006)] X; vzEx166 [Pdaf-7::trx-1::trx-1 3'-UTR; Punc-122::DsRed]*	This study

GF95	*trx-1(ok1449) II*; *Ex060 [skn-1(S74,340A)b/c::gfp; rol-6(su1006)]*	This study
GF96	*nsy-1(ok593) II*; *trx-1(ok1449) II*; *Is007 [skn-1b/c::gfp; rol-6(su1006)] X*	This study
GF97	*trx-1(ok1449) II*; *sek-1(km4) X*; *Is007 [skn-1b/c::gfp; rol-6(su1006)] X*	This study
GF98	*trx-1(ok1449) II*; *pmk-1(km25) IV*; *Is007 [skn-1b/c::gfp; rol-6(su1006)] X*	This study
GF99	*trx-1(ok1449) II; Is007 [skn-1b/c::gfp; rol-6(su1006)] X; ofEx416 [Ptrx-1::trx-1::gfp; Punc-122::DsRed]*	This study
GF100	*trx-1(ok1449) II; Is007 [skn-1b/c::gfp; rol-6(su1006)] X; ofEx419 [Ptrx-1::trx-1(SGPS)::gfp; Punc-122::DsRed]*	This study

REFERENCES

1. Miranda-Vizuete, A., et al., *Lifespan decrease in a Caenorhabditis elegans mutant lacking TRX-1, a thioredoxin expressed in ASJ sensory neurons.* FEBS Lett, 2006. **580**(2): p. 484-90.

2. Link, C.D. and C.J. Johnson, *Reporter transgenes for study of oxidant stress in Caenorhabditis elegans.* Methods Enzymol, 2002. **353**: p. 497-505.

3. An, J.H. and T.K. Blackwell, *SKN-1 links C. elegans mesendodermal specification to a conserved oxidative stress response.* Genes Dev, 2003. **17**(15): p. 18   -93.

4. Inoue, H., et al., *The C. elegans p38 MAPK pathway regulates nuclear localization of the transcription factor SKN-1 in oxidative stress response.* Genes Dev, 2005. **19**(19): p. 2278-83.

5. Fierro-Gonzalez, J.C., et al., *The thioredoxin TRX-1 modulates the function of the insulin-like neuropeptide DAF-28 during dauer formation in Caenorhabditis elegans.* PLoS One, 2011. **6**(1): p. e16561.

Table S5. Primers used for qRT-PCR.

snb-1 F	CCGGATAAGACCATCTTGACG
snb-1 R	GACGACTTCATCAACCTGAGC
gst-4 F	CGTTTTCTATGGAAGTGACGC
gst-4 R	TCAGCCCAAGTCAATGAGTC
gst-7 F	GGACAAGACTTCGAGGACAAC
gst-7 R	AACTGACGAGCCAAGTAACG
gst-9 F	TCTCGGTGACCAATTCAAGG
gst-9 R	AAGCCGGAACGAATAAATCTTTG
gst-10 F	AAGAGATTGTGCAGACTGGAG
gst-10 R	AGAACATGTCGAGGAAGGTTG
gst-12 F	TTTTGGAGATGGAAGCTGGG
gst-12 R	TTTTCCAGCGAACCCGAA
gst-14 F	TTGAGGATGAACGGGTGAAC
gst-14 R	TCTAGCAAGGTAGCGATTTATGG
gst-19 F	TGATTGCCCGTTTAAAGATGAAC
gst-19 R	ATTTCAGAGCAAGGTAGCGG
gst-36 F	GTTTTGAAATCCGAGATGCCG
gst-36 R	ATATCCAAGCGAGCACAGTC
gst-38 F	TCAACGGAAAGAGCAGATGG
gst-38 R	CGTCTCCTTCTGTGTAACCAAG
gst-44 F	GCAGAAAGTCTACTGGAAGGAG
gst-44 R	AAGTTGTCCGATGGAAGTGG
vit-4 F	AGAGCATCACACCATTGAGAG
vit-4 R	GATTGGGCGAGTTGGATAAGA
vit-5 F	CTACGAGAGCAACTACGATGAAA
vit-5 R	CTCCTTGATGAGGGTCTTCTTG
col-81 F	TAGCAACTCAGTGGGCTATTG
col-81 R	ATGCTGGAATTGAGAGGGATATT
col-137 F	ACGTCATACCGGACAAATGAA
col-137 R	CATTCCCATCCTCGTCAACATA
col-140 F	GATACCTGGAACCGTGTTGT
col-140 R	GCGAGATCTACGAATACCGAAA
skpo-1 F	GGACAACTGTATCGTACACCAG
skpo-1 R	CCATCACGGAGTCTCTCAAA
lbp-8 F	TCAGTCCTTCCTTATGGTTTCC
lbp-8 R	AGACCAACTCCGATTTCTTTCA
lips-6 F	TGCCAACTATCCACGACAATAC
lips-6 R	TGTCCCAAACAGTCAACTTACA
lips-11 F	TTCAGCATAGACAAGCGAGTAG
lips-11 R	GTATGGAATGGTGTAGGGATCTG

Table S6. log2fold changes of genes from RNA Seq Analysis. Sheet 1 (wtPlus_wtMinus): log2fold changes of genes in stressed wild type N2 animals, as compared to unstressed wild type N2 animals. Sheet 2 (*trx-1*Plus_*trx-1*Minus): log2fold changes of genes in stressed *trx-1* mutants, as compared to unstressed *trx-1* mutants. Sheet 3 (wtMinus_*trx-1*Minus): log2fold changes of genes in unstressed *trx-1* mutants, as compared to unstressed wild type N2 animals. Sheet 4 (wtPlus_*trx-1*Plus): log2fold changes of genes in stressed *trx-1* mutants, as compared to stressed wild type N2 animals. (.xlsm, 65 KB)

Available for download as a .xlsm file at
www.genetics.org/lookup/suppl/doi:10.1534/genetics.115.185272/-/DC1/TableS6.xlsm